



Evaluating the phytotoxicological effects of bulk and nano forms of zinc oxide on cellular respiration-related indices and differential gene expression in *Hordeum vulgare* L.

Kirill Azarin^a, Alexander Usatov^a, Tatiana Minkina^a, Nadezhda Duplii^a, Aleksei Fedorenko^a, Andrey Plotnikov^a, Saglara Mandzhieva^a, Rahul Kumar^b, Jean Wan Hong Yong^{c,*}, Shafaque Sehar^{d,*}, Vishnu D. Rajput^{a,*}

^a Southern Federal University, Rostov-on-Don 344090, the Russian Federation

^b Chitkara Centre for Research and Development, Chitkara University, Himachal Pradesh 174103, India

^c Department of Biosystems and Technology, Swedish University of Agricultural Sciences, Alnarp 23456, Sweden

^d Department of Agronomy, College of Agriculture and Biotechnology, Zhejiang University, Hangzhou 310058, China

ARTICLE INFO

Edited by Dr. Muhammad Zia-ur-Rehman

Keywords:

Barley
Mitochondria
Nanoparticles
Oxidative phosphorylation
ROS
Ultrastructure
Zinc

ABSTRACT

The increasing use of nanoparticles is driving the growth of research on their effects on living organisms. However, studies on the effects of nanoparticles on cellular respiration are still limited. The remodeling of cellular-respiration-related indices in plants induced by zinc oxide nanoparticles (nnZnO) and its bulk form (blZnO) was investigated for the first time. For this purpose, barley (*Hordeum vulgare* L.) seedlings were grown hydroponically for one week with the addition of test compounds at concentrations of 0, 0.3, 2, and 10 mg mL⁻¹. The results showed that a low concentration (0.3 mg mL⁻¹) of blZnO did not cause significant changes in the respiration efficiency, ATP content, and total reactive oxygen species (ROS) content in leaf tissues. Moreover, a dose of 0.3 mg mL⁻¹ nnZnO increased respiration efficiency in both leaves (17 %) and roots (38 %). Under the influence of blZnO and nnZnO at medium (2 mg mL⁻¹) and high (10 mg mL⁻¹) concentrations, a dose-dependent decrease in respiration efficiency from 28 % to 87 % was observed. Moreover, the negative effect was greater under the influence of nnZnO. The gene transcription of the subunits of the mitochondria electron transport chain (ETC) changed mainly only under the influence of nnZnO in high concentration. Expression of the ATPase subunit gene, *atp1*, increased slightly (by 36 %) in leaf tissue under the influence of medium and high concentrations of test compounds, whereas in the root tissues, the *atp1* mRNA level decreased significantly (1.6–2.9 times) in all treatments. A dramatic decrease (1.5–2.4 times) in ATP content was also detected in the roots. Against the background of overexpression of the *AOX1d1* gene, an isoform of alternative oxidase (AOX), the total ROS content in leaves decreased (with the exception of 10 mg mL⁻¹ nnZnO). However, in the roots, where the pressure of the stress factor is higher, there was a significant increase in ROS levels, with a maximum six-fold increase under 10 mg mL⁻¹ nnZnO. A significant decrease in transcript levels of the pentose phosphate pathway and glycolytic enzymes was also shown in the root tissues compared to leaves. Thus, the disruption of oxidative phosphorylation leads to a decrease in ATP synthesis and an increase in ROS production; concomitantly reducing the efficiency of cellular respiration.

1. Introduction

Nanotechnology is the branch of science and engineering that focuses on understanding and control of materials on the molecular, atomic, or even subatomic scale. More recently, this technology is gaining recognition because of its numerous applications in many

sectors, including medicine, geology, chemistry, optics, catalysis, electronics and agriculture (Barhoum et al., 2022; Elmer and White, 2018; Fincheira et al., 2021; Jalil et al., 2023a; Khan et al., 2022; Pang et al., 2024; Piccinno et al., 2012; Sani et al., 2023; Nam and Luong, 2019). Specifically, the application of nanotechnology in agriculture has undeniable benefits to improve production efficiency, physiological

* Corresponding authors.

E-mail addresses: jean.yong@slu.se (J.W.H. Yong), shafaquesehar@yahoo.com (S. Sehar), rvishnu@sfnu.ru (V.D. Rajput).

<https://doi.org/10.1016/j.ecoenv.2024.116670>

Received 27 March 2024; Received in revised form 26 June 2024; Accepted 28 June 2024

Available online 8 July 2024

0147-6513/© 2024 The Author(s). Published by Elsevier Inc. This is an open access article under the CC BY license (<http://creativecommons.org/licenses/by/4.0/>).

resilience and sustainability of crops (Adil et al., 2024; Alhathloul et al., 2023; Haider et al., 2024; Hanif et al., 2024; Jalil et al., 2023b). For instance, the use of essential metal nanoparticles as fertilizers allows for a reduction in the amount of substances applied while ensuring high physiological efficiency (Tombuloglu et al., 2019a; Al-Amri et al., 2020). One such nano-fertilizer can be the ZnO nanoparticles. At a low concentration (0.05 mg mL^{-1}), ZnO nanoparticles contributed to increased biomass and stress resistance in *Oryza sativa* seedlings (Singh et al., 2018). ZnO nanoparticles at a concentration of 0.1 mg mL^{-1} promoted the accumulation of potassium and iron, as well as increased biomass in *Datura stramonium* (Vafae Moghadam et al., 2022). Long-term application of ZnO nanoparticles (0.05 mg mL^{-1}) activated nitrate reductase, increased growth rate, and biomass accumulation in *Glycine max* (Mirakhorli et al., 2021). Spraying *Triticum aestivum* with ZnO nanoparticles at a dose of 0.01 mg mL^{-1} led to the remobilization of nutrients, an increase in seed mass, and the number of spikelets (Niazi et al., 2023). Foliar application (0.003 mg mL^{-1}) also increased the growth rate, biomass accumulation, and yield in *Solanum lycopersicum* (Pejam et al., 2021). Treating seeds with 0.01 mg mL^{-1} ZnO nanoparticles led to an increase in chlorophyll content and photosynthesis efficiency in adult *Triticum aestivum* plants (Rai-Kalal and Jajoo, 2021). An increase in the amount of photosynthetic pigments, photosynthesis efficiency, and consequently biomass was shown when treated with low doses of ZnO nanoparticles in *Saccharum officinarum* (Elsheery et al., 2020), *Trigonella foenum-graecum* (Chemingui et al., 2019), and *Coffea arabica* (Rossi et al., 2019).

On the other hand, it has been shown that ZnO nanoparticles at levels above 0.1 mg mL^{-1} exhibited a toxic effect (Nair and Chung, 2017; Chen et al., 2018; Molnár et al., 2020; Ahmed et al., 2021). A decrease in morphometric parameters and photosynthetic pigments was shown in *Arabidopsis thaliana* when treated with ZnO nanoparticles at 0.3 mg mL^{-1} (Wang et al., 2016). ZnO nanoparticles at $0.05\text{--}1 \text{ mg mL}^{-1}$ concentration range disrupted the root cell formation in *Lolium perenne* (Lin and Xing, 2008). Doses from 0.25 mg mL^{-1} to 1 mg mL^{-1} caused oxidative stress in *Abelmoschus esculentus* (Baskar et al., 2021). Chromosome aberrations were shown when *Alium cepa* was exposed to 0.5 mg mL^{-1} and 1 mg mL^{-1} ZnO nanoparticles (Ahmed et al., 2017). Doses of 0.5 mg mL^{-1} and 1 mg mL^{-1} also caused DNA damage in *Triticum aestivum* (Zhu et al., 2019). A dose-dependent decrease in morphophysiological parameters, secondary metabolites and activity of the antioxidant system was shown when *Stevia rebaudiana* was treated with ZnO nanoparticles at concentrations of 0.1 mg mL^{-1} and 1 mg mL^{-1} (Javed et al., 2017). Modulation of the phytotoxic effect of ZnO nanoparticles at concentrations ranging from 0.3 mg mL^{-1} to 1.2 mg mL^{-1} has been studied in *T. aestivum* (Iftikhar et al., 2019). Concentrations of $0.5, 1,$ and 1.5 mg mL^{-1} caused a decrease in biomass and an increase in lipid peroxidation in *Brassica juncea* (Rao and Shekhawat, 2014). It was shown in six plant species that ZnO nanoparticles at a concentration of 2 mg mL^{-1} inhibited seed germination and further plant growth (Lin and Xing, 2007). A dose of 2 mg mL^{-1} caused a reduction in shoot elongation in *Zea mays* and root elongation in *Z. mays* and *Oryza sativa* (Yang et al., 2015). Salehi et al. (2021) found that at a low dose (0.25 mg mL^{-1}) ZnO nanoparticles caused an increase in proteins and secondary metabolites associated with stress and antioxidant defense, while a high dose (2 mg mL^{-1}) suppressed the antioxidant system and led to oxidative damage in *Phaseolus vulgaris*. Also, a study of the effect of ZnO nanoparticles ($0.25\text{--}2 \text{ mg mL}^{-1}$) showed a dose-dependent decrease in viability and an increase in abnormality of pollen in *P. vulgaris* (Salehi et al., 2022). ZnO nanoparticles at concentrations of $0.4, 2$ and 4 mg mL^{-1} demonstrated higher phytotoxic effects on *A. thaliana* compared to some other heavy metal oxide nanoparticles (Lee et al., 2010). López-Moreno et al. (2010) using ZnO nanoparticle concentrations of $0.5, 2,$ and 4 mg mL^{-1} showed various effects on *Glycine max*, including the disruption of DNA integrity. Mediated changes in the nutritional status, phytohormones, antioxidant status, and membrane integration in plants can occur due to the disruption of the soil

microbiome by ZnO nanoparticles (Iranbakhsh et al., 2021). These rhizospheric perturbations were likely to alter the microbial population and activity, as well as the inhibition of important microorganisms for plants such as *Azotobacter* and P- and K-solubilizing bacteria.

From the environmental management perspectives, ZnO nanoparticles possess a high potential for contamination and can accumulate in soil and surface waters under certain scenarios (Adil et al., 2024; Gottschalk et al., 2009; Jan et al., 2022; Song et al., 2010; Wan et al., 2019). Boxall et al. (2007) found, based on the production data of cosmetics and personal care products, that the concentration of ZnO nanoparticles in soil was up to 0.03 mg mL^{-1} , and in sludge was up to 21 mg mL^{-1} . Such an increase in the utility of nanoparticles in various fields - especially agriculture, in the form of pesticides and fertilizers - inevitably leads to their penetration of and accumulation in plants, which carries certain environmental risks (Kang et al., 2023).

Cellular respiration is a chain of complex biochemical reactions that transforms the oxidation energy of organic substances into macroergic molecules, such as ATP. The optimal functioning of cellular respiration contributes to the resilience of plants during unfavorable periods. During the same time frame, the links of the respiratory chain can be immediate or indirect objectives of abiotic factors. Mitochondria, in which cellular respiration occurs, are the core source of reactive oxygen species (ROS) in the cell, participate in redox signaling and can be involved in the general response to stress caused by nanoparticles (Keunen et al., 2011). In turn, a decrease in energy metabolism causes a decline in agricultural yield, which is a global environmental risk. Several studies have revealed the effect of heavy-metal nanoparticles on the plant cellular respiration. Increased respiration was shown when exposed to HgO nanoparticles in *Z. mays* and *T. aestivum* (Abdelgawad et al., 2020). Overactivation of the tricarboxylic cycle was also revealed in *Cucumis sativus* under Ag nanoparticle exposure (Zhang et al., 2018). A rise in the amount of the mitochondrial membrane potential and apoptosis were caused by the impact of Co_3O_4 nanoparticles on *Solanum melongena* (Faisal et al., 2016). A significant change in the mitochondrial membrane potential was detected in plant cells when exposed to ZnO nanoparticles (Ahmed et al., 2017). Disturbances in the electron transport chain were observed when CuO nanoparticles were exposed to tobacco cell cultures (Dai et al., 2018). A proteomic analysis revealed a reduction in the expression of proteins in the mitochondrial electron transfer chain after treating *T. aestivum* seedlings with Ag nanoparticles (Jhazab et al., 2019). Prolonged exposure to CuO nanoparticles significantly inhibited respiration in the microalgae *Chlorella sp.* and *Scenedesmus sp.* (Che et al., 2018). Thus, a considerable reorganization of plant respiration due to heavy-metal nanoparticles exposure was shown. However, various molecular and physiological aspects of their effect on respiration have not been sufficiently studied. Moreover, there are no studies on the impact of ZnO nanoparticles on the cellular respiration of higher plants. Thus, this study aims to investigate several key aspects related to ZnO nanoparticles and plant respiration: i) to investigate the dose-dependent and size-dependent effects of bulk and nano ZnO on the efficiency of cellular respiration and ATP content in barley leaves and roots, ii) to assess the impact of bulk and nano ZnO on the accumulation of reactive oxygen species (ROS) in barley tissues and changes in the ultrastructure of mitochondria in barley leaves and roots, and iii) to analyze the differential gene expression related to mitochondrial electron transport chain components and oxidative phosphorylation in barley seedlings treated with bulk and nano ZnO. It has been hypothesized that ZnO nanoparticles can have phytotoxicological effects on plant's energy metabolism, and the functioning of the plant cellular respiration system was examined under the action of bulk (bZnO) and nano (nnZnO) forms of zinc oxide on barley seedlings.

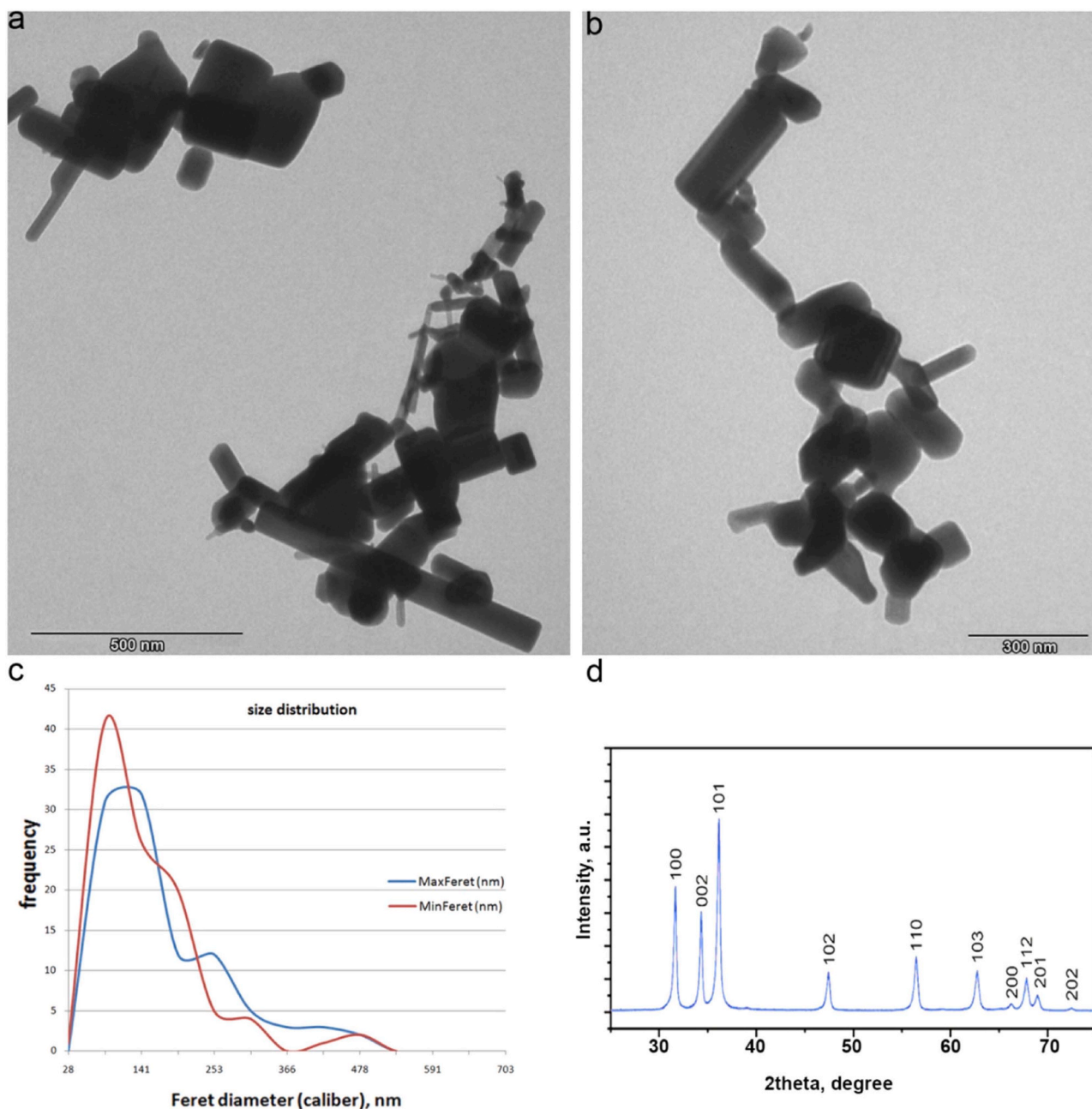


Fig. 1. Characterization of ZnO nanoparticles; (a, b) TEM image, (c) size distribution, (d) X-ray diffraction pattern.

2. Materials and methods

2.1. Plant material, zinc oxide NPs characterization and treatment application

The plant material used in the study was barley seedlings (*Hordeum vulgare* L.) of the Medium157 cultivar. Initially, the seeds were disinfected with a 1 % NaClO solution. The seeds were then washed with distilled water and germinated on damp filter paper. Germination was carried out for 36 h at a temperature of 25 ° C. Next, the germinated seeds with the same growth energy were selected and transferred to plastic reservoirs with blZnO or nnZnO suspensions at concentrations of 0.3 mg mL⁻¹, 2 mg mL⁻¹, and 10 mg mL⁻¹. Zinc oxide nanoparticles were commercially obtained from Aldrich, USA, and had an elongated shape with clear edges (Fig. 1a, b). The largest proportion of particles had a Minimum Feret Diameter (minFeret) of 60±4 nm and a Maximum

Feret Diameter (maxFeret) of 132±8 nm. (Fig. 1c).

The results of X-ray diffraction analysis showed the standard peaks and the high purity of the studied compound (Fig. 1d). Previous measurements of the ζ-potential (22 mV – -6.5 mV) demonstrated the stability of the ZnO nanoparticle colloidal system (Rajput et al., 2021; Voloshina et al., 2022). Fourier-transform infrared spectroscopy confirmed the presence of the ZnO functional group in the samples (Voloshina et al., 2022). The choice of doses of 0.3 mg mL⁻¹ and 2 mg mL⁻¹ was based on numerous phyto-toxicological studies of nnZnO (Kang et al., 2023) as well as the existing levels of Zn pollution of soils in the industrial parts of the Rostov area (Minkina et al., 2017). The dose of 10 mg mL⁻¹ was used as destructive for agricultural crops (Rajput et al., 2018; Hayat et al., 2020). During the experiment, constant temperature (25 ° C), illumination (300–400 μmol m⁻² s⁻¹) and photoperiod (16/8 h) were maintained. After 7 days, the biochemical analysis and the gene expression level involved in respiration were

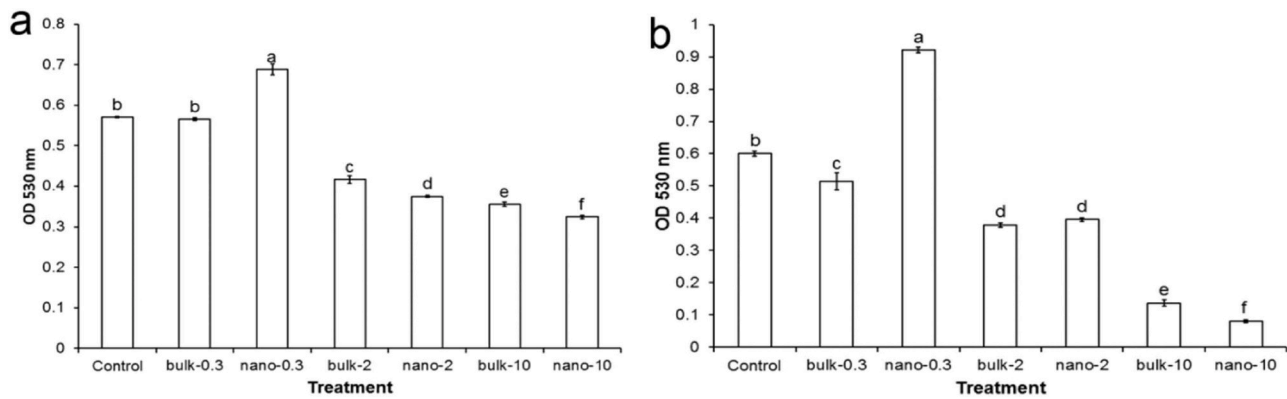


Fig. 2. Respiratory efficiency in the (a) leaves and (b) roots of barley under blZnO and nnZnO treatments. Different letters on the columns refer to statistically significant differences at $P \leq 0.05$.

carried out.

2.2. Evaluation of respiratory activity

Respiratory activity in barley tissue was evaluated using 2,3,5-triphenyltetrazolium chloride (Marmiroli et al., 2020). A 100-mg portion of the plant tissue was immersed in 1.5 mL of phosphate buffer (pH 7.4) containing 0.18 M 2,3,5-triphenyltetrazolium chloride and kept at 25 °C for 24 h. After three-fold washings with deionized water, extraction with ethanol (95 %) of the formazan formed as a result of the reduction of 2,3,5-triphenyltetrazolium chloride was carried out. Quantitative determination was conducted on a spectrophotometer (SmartSpec Plus, Bio Rad) at a wavelength of 530 nm.

2.3. Determination of ATP content

The ATP content in the samples was determined fluorimetrically using the ATP Assay Kit (Sigma-Aldrich) following the manufacturer's instructions. Fresh samples were homogenized in liquid nitrogen, dissolved in ATP Assay Buffer at a ratio of 10 mg tissue to 100 μ L of buffer and deproteinized with a 10 kDa Molecular Weight Cut Off (MWCO) spin filter. Next, the samples were incubated with the appropriate Reaction Mix for 30 min and the fluorescence was recorded ($\lambda_{ex} = 535/\lambda_{em} = 587$ nm). ATP concentration was expressed in μ g g^{-1} FW according to the standard curve.

2.4. Determination of ROS level

The total pool of ROS was determined through a fluorescent test based on the formation of dichlorofluorescein from non-fluorescent dichlorofluorescein-diacetate (Kozel and Shalygo, 2009). A 0.5 g sample of fresh plant material was crushed in liquid nitrogen with the addition of 2 mL of 0.2 N HClO₄ and subsequent neutralization with 37 μ L of 4 M KOH. Next, 950 μ L of 0.15 M Tris-HCl buffer (pH 7.5), 25 μ L of supernatant and 25 μ L of 0.5 mM dichlorofluorescein-diacetate solution were added sequentially. The samples were stored in a thermostat at 37 °C for 20 min, after which the fluorescence spectra were recorded ($\lambda_{ex} = 496$ nm/ $\lambda_{em} = 524$ nm) on a RF-5301 spectrofluorimeter (Shimadzu). The ROS content was calculated in μ g g^{-1} FW.

2.5. Mitochondria isolation and zinc quantification

Isolation of the mitochondria from roots and leaves was carried out using 1 g of tissue homogenate in 5 mL Tris-HCl buffer (pH 7.5) with a series of increasing centrifugations (AvantiJ-HC, BeckmanCoulter, USA) according to the following methodology (Salvato et al., 2014; Lysenko et al., 2019). The zinc content in tissues and isolated mitochondria was determined using KVANT 2-ATatomic absorption spectrophotometry

(KartaLtd, Russian) as previously described (Azarin et al., 2022).

2.6. Ultrastructural analysis

For microscopic examination, cuttings (2×2 mm) from leaf and root tissue were taken and fixed in a 2.5 % solution of glutaraldehyde in a phosphate buffer (pH 7.4) for 4 h at room temperature. After washing three times with phosphate buffer and additional fixation with a 2 % OsO₄ solution, the tissues were dehydrated with ethanol and kept in a 70 % alcohol solution of uranyl acetate for 12 hours in the cold (4 °C). The tissues were then washed from uranyl acetate and additionally dehydrated in 96 % and 100 % ethanol and pure acetone (100 %). The samples were impregnated with resin in a series of Epon solutions in acetone of increasing concentrations and poured into Epon. Polymerization was carried out in a thermostat at a temperature of 37 °C (24 h), 48 °C (24 h), 60 °C (48 h). Morphometric analysis of electron microscopic images of the mitochondria involved counting the quantity of sectional areas and membrane lengths. The coefficient of energetic efficiency of the mitochondria was calculated as the multiplication of the average total number of cristae per cell and the average area of all mitochondria in the same cell (Paukov et al., 1971). For morphometric measurements, a micrograph analysis system Olympus Soft Imaging Solution ITEM was used.

2.7. Gene expression analysis

To isolate total RNA from plant tissue, guanidine thiocyanate-phenol-chloroform extraction was used (Chomczynski and Sacchi, 1987) with variations (Azarin et al., 2020). Reverse transcription was conducted with the use of the MMLVkit (Evrogen, Russia) and 4 μ L of RNA from each sample. Real-time polymerase chain reaction (qPCR) was performed in a QuantStudio 5 thermal cycler (AppliedBiosystems) with the use of SYBRGreenI (Evrogen, Russia) and specific primers (Table S1). The $2^{-\Delta\Delta Ct}$ method (Livak and Schmittgen, 2001) was used to calculate the quantitative changes in gene expression.

2.8. Statistical analyses

The data analysis from the outcomes of six independent repeats was carried out using Excel. The reliability of the data obtained was assessed by analysis of variance (ANOVA) with the Tukey test ($P < 0.05$). The correlation heat map was generated using ChiPlot (<https://www.chiplot.online/>).

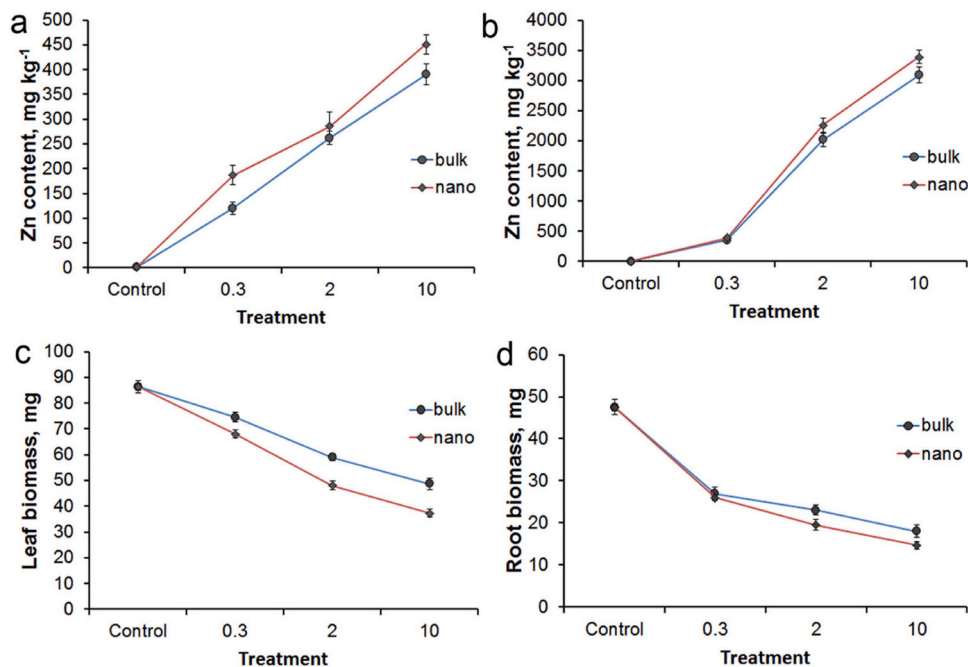


Fig. 3. Bioaccumulation of zinc in (a) leaves and (b) roots; biomass of (c) leaves and (d) roots under blZnO and nnZnO treatments.

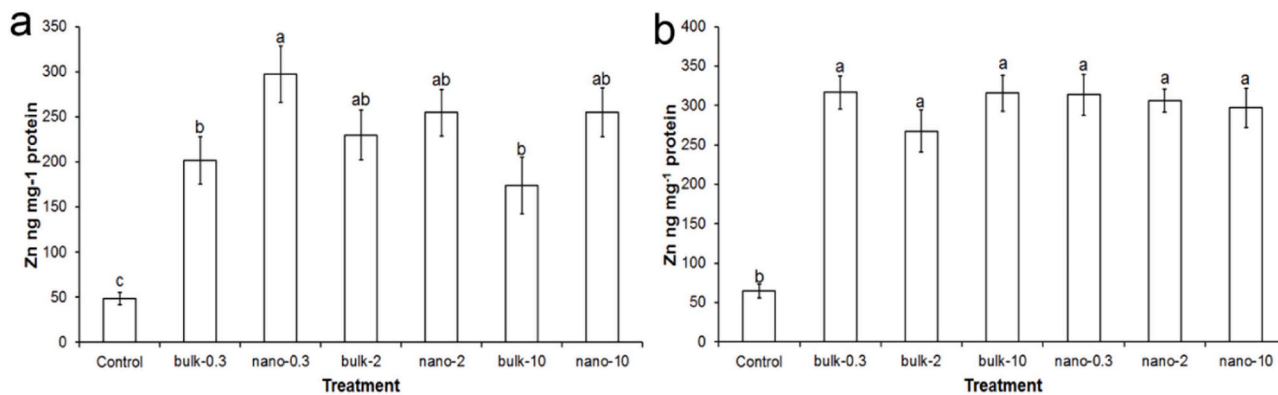


Fig. 4. Zinc content in the mitochondria of the (a) leaves and (b) roots under blZnO and nnZnO treatments. Different letters on the columns refer to statistically significant differences at $P \leq 0.05$.

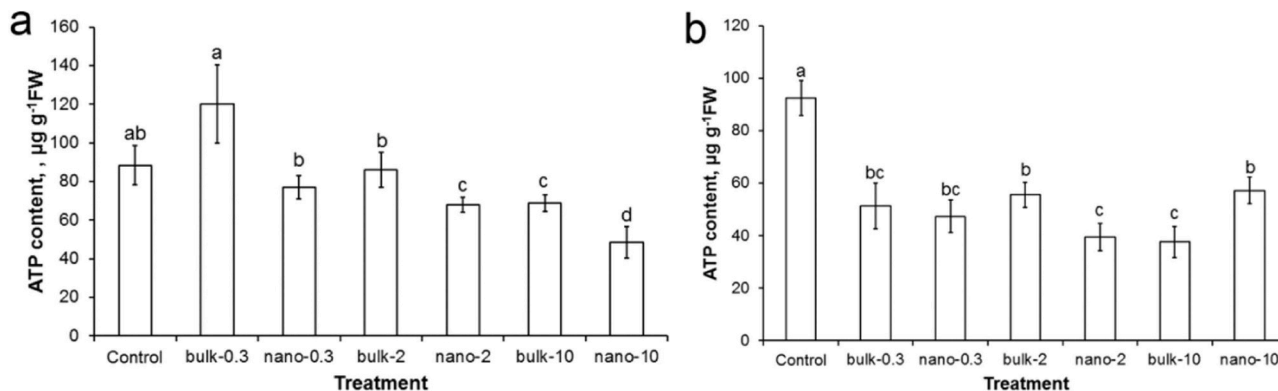


Fig. 5. ATP content in the (a) leaves and (b) roots of barley under blZnO and nnZnO treatments. Different letters on the columns refer to statistically significant differences at $P \leq 0.05$.

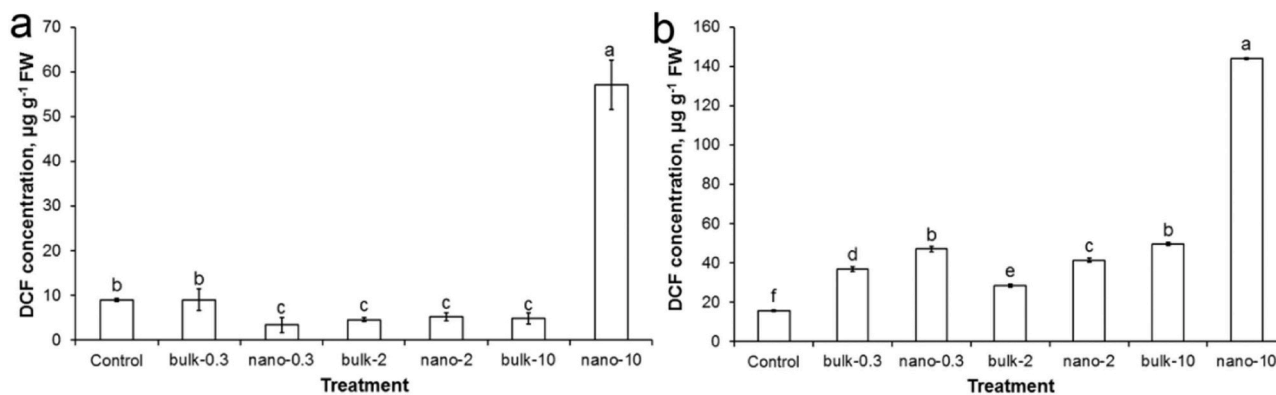


Fig. 6. Total ROS level in the (a) leaves and (b) roots of barley under blZnO and nnZnO treatments. Different letters on the columns refer to statistically significant differences at $P \leq 0.05$.

3. Results

3.1. Respiration efficiency

A significant change in respiration efficiency in the leaf and root cells of blZnO- and nnZnO-treated barley seedlings was shown by measuring reduced 2,3,5-triphenyltetrazolium chloride (Fig. 2b). The smallest decrease (15 %) in the respiration index in root cells was revealed under the influence of 0.3 mg mL^{-1} blZnO, and the largest decreases (78 % and 87 %) were shown when treated with blZnO and nnZnO at a concentration of 10 mg mL^{-1} . In leaf cells, the greatest suppression of respiration efficiency, by 38 % and 45 %, was caused by 10 mg mL^{-1} blZnO and nnZnO, respectively. Treatment with 0.3 mg mL^{-1} blZnO did not affect the respiration, and 0.3 mg mL^{-1} nnZnO increased the index by 17 % (Fig. 2a).

3.2. Zinc accumulation and plant biomass

Bioaccumulation of zinc in leaf and root tissues demonstrated a dose-dependent increase (Fig. 3a, b). As expected, the zinc content in the roots was higher than in the leaves. In parallel with the increase in zinc in the seedling organs, a reduction in their biomass occurred (Fig. 3c, d). It is worth noting that a greater accumulation of zinc under the influence of nnZnO was associated with a greater reduction of biomass.

3.3. Mitochondrial zinc content

Analysis of the zinc content showed a significant increase compared to the control, both in the mitochondria of the leaves and roots in all treatment options (Fig. 4). However, the dependence of such an increase on the dosage or size of the applied zinc oxide was not revealed.

3.4. ATP content

The study of the ATP content revealed its decrease in root tissues with all treatments (Fig. 5b). The greatest decrease (by 2.4 times) was shown when exposed to blZnO at a concentration of 10 mg mL^{-1} . In leaf cells, the doses of 10 mg mL^{-1} blZnO and 2 mg mL^{-1} nnZnO led to a decrease in the ATP content by 23 %, while 10 mg mL^{-1} nnZnO reduced the ATP content by 46 %. In other treatment options, the ATP content did not change relative to the control (Fig. 5a).

3.5. Total ROS level

An increase in the total ROS in root cells was registered when exposed to blZnO and nnZnO in all concentrations studied, while at the same dosage, the nanodisperse form had a greater effect than the macrodisperse form of ZnO (Fig. 6b). In leaf cells, 0.3 mg mL^{-1} blZnO did not change the total ROS content relative to the control. The doses of 2 mg mL^{-1} blZnO, 10 mg mL^{-1} blZnO, 0.3 mg mL^{-1} nnZnO and 2 mg mL^{-1} nnZnO led to a decrease in the ROS pool from 1.7 to 2.7

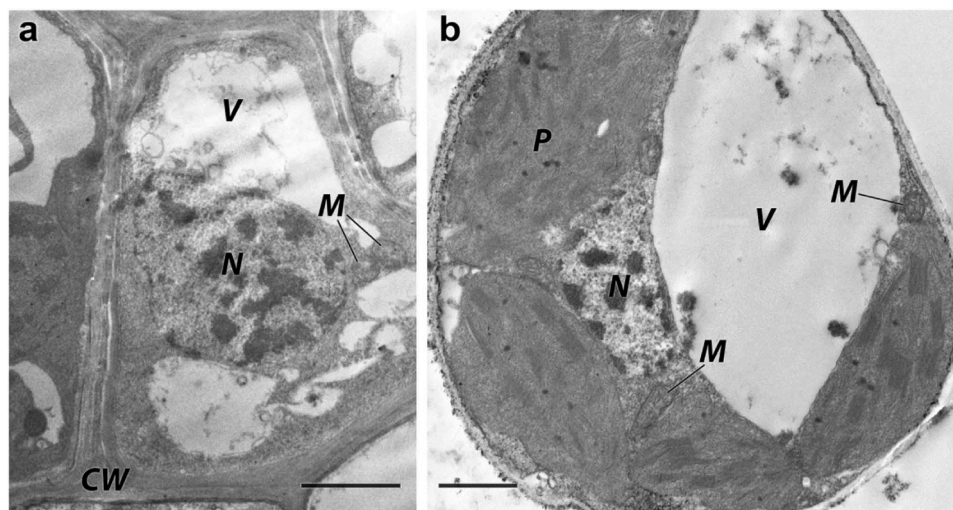


Fig. 7. TEM image of (a) root cell and (b) leaf cell of barley. Control, general view: CW - cell wall, M - mitochondrion, N - nucleus, P - plastid, V - vacuole. Bars (a) 2 µm, (b) 1 µm.

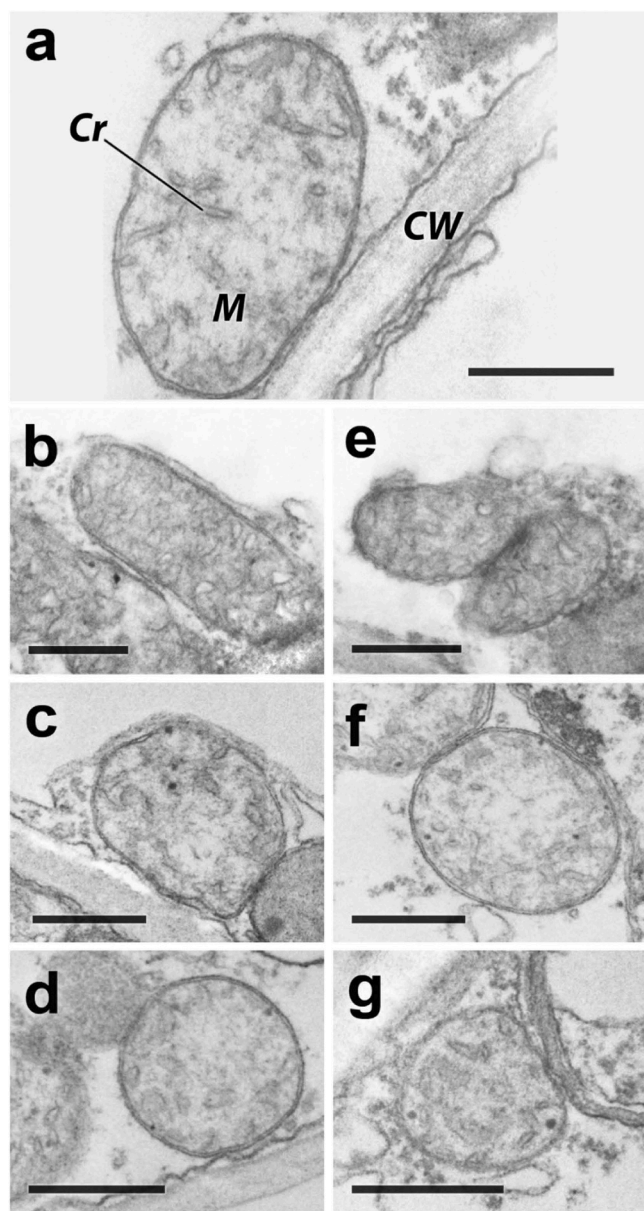


Fig. 8. Ultrastructure of barley leaf mitochondria under blZnO and nnZnO treatments. **a** - control; **b** - 0.3 mg mL^{-1} blZnO; **c** - 2 mg mL^{-1} blZnO; **d** - 10 mg mL^{-1} blZnO; **e** - 0.3 mg mL^{-1} nnZnO; **f** - 2 mg mL^{-1} nnZnO; **g** - 10 mg mL^{-1} nnZnO. **CW**, cell wall; **Cr**, crista; **M**, mitochondria. **Bars** $0.5 \mu\text{m}$.

times, while 10 mg mL^{-1} nnZnO caused an increase by more than six times (Fig. 6a).

3.6. Ultrastructural analysis

In the control, the mitochondria, in both the roots and the leaves were oval in shape and contained an electron-light matrix and well-defined cristae (Fig. 7). Exposure to blZnO and nnZnO caused alterations in the mitochondria in the seedlings (Figs. 8, 9). The mitochondria became heterogeneous especially when exposed to high concentrations. Some organelles were compacted, while others were swollen with destroyed cristae. The number of mitochondria per cell, their average size, and the ratio of the length of the contour of the inner membrane to the outer one decreased with increased concentrations of the introduced pollutant (Tables 1, 2). The greatest decrease was observed under the influence of the nnZnO at the maximum concentration. In the roots, under the influence of 10 mg mL^{-1} nnZnO, the

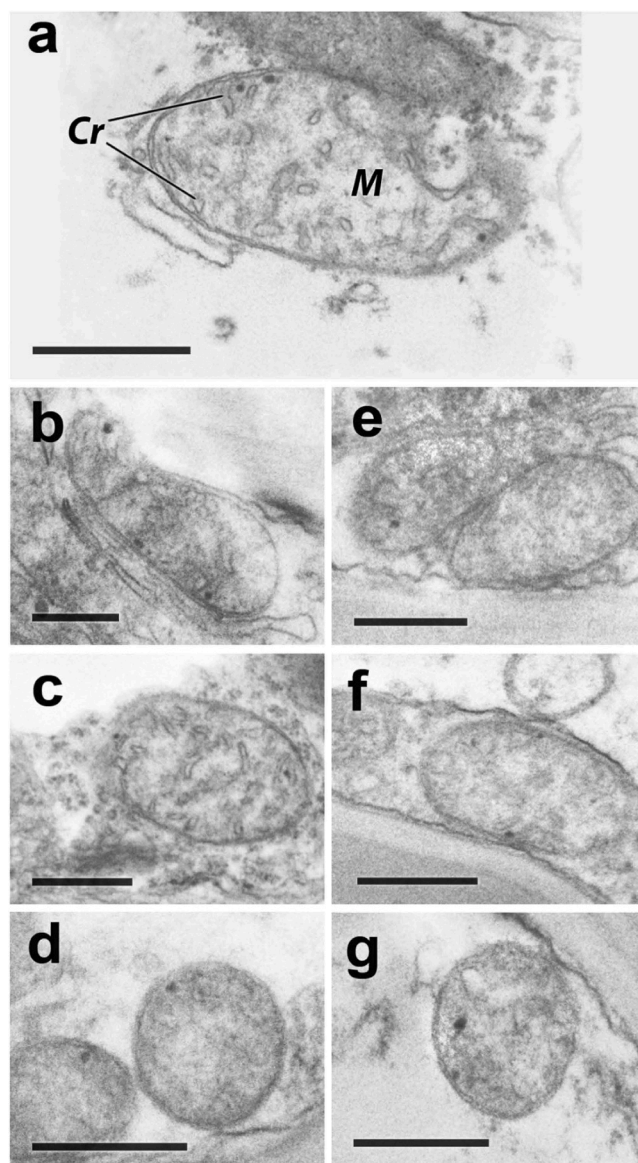


Fig. 9. Ultrastructure of barley root mitochondria under blZnO and nnZnO treatments. **a** - control; **b** - 0.3 mg mL^{-1} blZnO; **c** - 2 mg mL^{-1} blZnO; **d** - 10 mg mL^{-1} blZnO; **e** - 0.3 mg mL^{-1} nnZnO; **f** - 2 mg mL^{-1} nnZnO; **g** - 10 mg mL^{-1} nnZnO. **Cr**, crista; **M**, mitochondria. **Bars** $0.5 \mu\text{m}$.

number of mitochondria decreased by 26.2 %, and their area was reduced by 40 %. In leaves, 10 mg mL^{-1} nnZnO reduced the number of mitochondria by 43.7 %, and their area by 43.5 %. The degree of change in membrane structures had a non-linear pattern. Thus, at the low concentration of the pollutants, the internal membranes showed higher values of indices than in the control, and with an increase in the concentration of the pollutant, the membrane indices decreased. However, the increase in the membrane apparatus was compensated by a decrease in the average size of the mitochondria and their number, which was reflected in a dose-dependent decrease in the coefficient of energetic efficiency, which characterizes the energy-forming capacity of the mitochondria (Tables 1 and 2).

3.7. Respiration-related gene expression

The study of the genes encoding the subunits of the transmembrane protein complexes of the mitochondrial electron transport respiratory chain in treated barley seedlings revealed significant changes in their

Table 1
Quantitative fine-structural analysis of the mitochondria in barley leaf under blZnO and nnZnO treatments.

Treatment	Number of mitochondria per cell	Average mitochondria area, μm^2	Number of cristae per mitochondria	Average crista area, μm^2	Proportion of the crista area in the mitochondria, %	Ratio of the contour length of the inner membrane to the outer one	Coefficient of energetic efficiency of the mitochondria
Control	8.8 ± 1.5 ^a	0.69 ± 0.07 ^a	19.2 ± 2.0 ^b	0.078 ± 0.015 ^a	11.5	2.05	957.9 ± 28.5 ^a
bulk-0.3	5.2 ± 1.1 ^b	0.53 ± 0.08 ^{ab}	23.8 ± 2.5 ^a	0.091 ± 0.028 ^a	17.4	1.99	341.6 ± 15.2 ^b
nano-0.3	5.4 ± 0.8 ^b	0.51 ± 0.05 ^b	22.4 ± 3.3 ^{ab}	0.089 ± 0.026 ^a	16.9	1.89	333.8 ± 11.4 ^b
bulk-2	5.6 ± 0.6 ^b	0.47 ± 0.07 ^b	16.3 ± 3.5 ^b	0.072 ± 0.021 ^a	15.1	1.89	240.1 ± 24.5 ^c
nano-2	5.1 ± 1.7 ^b	0.45 ± 0.06 ^b	15.8 ± 3.2 ^b	0.069 ± 0.023 ^a	14.8	1.88	185.3 ± 18.5 ^d
bulk-10	5.4 ± 1.3 ^b	0.41 ± 0.08 ^b	14.7 ± 5.0 ^b	0.057 ± 0.013 ^a	13.3	1.85	176.2 ± 18.4 ^{de}
nano-10	4.9 ± 1.3 ^b	0.39 ± 0.08 ^b	13.9 ± 3.7 ^b	0.052 ± 0.014 ^a	13.1	1.76	150.5 ± 9.4 ^e

Different letters on the columns refer to statistically significant differences at $P \leq 0.05$.

Table 2
Quantitative fine-structural analysis of the mitochondria in barley root under blZnO and nnZnO treatments.

Treatment	Number of mitochondria per cell	Average mitochondria area, μm^2	Number of cristae per mitochondria	Average crista area, μm^2	Proportion of the crista area in the mitochondria, %	Ratio of the contour length of the inner membrane to the outer one	Coefficient of energetic efficiency of the mitochondria
Control	5.5 ± 1.3 ^a	0.26 ± 0.05 ^a	10.3 ± 1.2 ^a	0.027 ± 0.009 ^a	12.2	1.61	78.2 ± 4.6 ^a
bulk-0.3	4.9 ± 1.4 ^a	0.21 ± 0.09 ^a	12.5 ± 2.2 ^a	0.031 ± 0.008 ^a	18.6	1.58	63.0 ± 8.9 ^b
nano-0.3	4.8 ± 1.5 ^a	0.20 ± 0.07 ^a	11.9 ± 3.7 ^a	0.029 ± 0.006 ^a	17.1	1.57	39.4 ± 10.7 ^c
bulk-2	4.8 ± 1.6 ^a	0.18 ± 0.05 ^a	9.3 ± 3.2 ^a	0.025 ± 0.012 ^a	16.3	1.48	37.8 ± 7.1 ^c
nano-2	4.7 ± 1.7 ^a	0.17 ± 0.06 ^a	9.1 ± 3.8 ^a	0.024 ± 0.013 ^a	15.6	1.46	34.2 ± 7.3 ^c
bulk-10	4.3 ± 1.3 ^a	0.16 ± 0.08 ^{ab}	8.4 ± 2.8 ^a	0.022 ± 0.013 ^a	13.7	1.43	24.9 ± 5.6 ^{cd}
nano-10	4.1 ± 1.2 ^a	0.15 ± 0.05 ^b	8.1 ± 2.1 ^a	0.021 ± 0.007 ^a	14.2	1.42	20.6 ± 5.2 ^d

Different letters on the columns refer to statistically significant differences at $P \leq 0.05$.

transcriptional activity compared to the control (Fig. 10). In leaf tissue, the dose of 10 mg mL⁻¹ blZnO and nnZnO significantly reduced the expression level of the mitochondrial *nad2* gene, which encodes the subunit of the NADH dehydrogenase complex of mitochondrial ETC. The decrease in the transcript number of the 51 kDa NADH dehydrogenase [ubiquinone] flavoprotein 1 subunit, encoded by the *NDUFV1* nuclear gene, occurs only under the action of nnZnO at a concentration of 10 mg mL⁻¹. In root tissues, the transcription of the *NDUFV1* gene was suppressed in all treatments, and the lowest level of expression was recorded when exposed to 10 mg mL⁻¹. On the other hand, the activity of *nad2* in root tissues was increased under the action of 10 mg mL⁻¹ nnZnO.

Analysis of the transcription level of the nuclear genes *CYC1* and *UCR1*, encoding the cytochrome *c1* and Rieske subunits of the multi-protein cytochrome-*bc1* complex of mitochondrial ETC, revealed the following patterns. In leaf tissue, *CYC1* and *UCR1* transcription were suppressed exclusively by nnZnO at a concentration of 10 mg mL⁻¹. Under the influence of the studied types of zinc oxide (2 mg mL⁻¹ and 10 mg mL⁻¹), there was a reduction in the amount of *UCR1* expression in the roots, while *CYC1* was characterized by an increase in expression by 1.5 times with 0.3 mg mL⁻¹ blZnO and nnZnO, and by 1.9 times when exposed to 10 mg mL⁻¹ nnZnO. Significant suppression of the transcriptional activity of the nuclear and mitochondrial genes, *COX5C* and *cox1*, encoding cytochrome *c* complex subunits, was shown in leaf tissue only under the impact of nnZnO. In the root tissues in the presence of the studied pollutants, the activity of *COX5C* increased, while the greatest effect (by 2.1 times) was caused by nnZnO at a concentration of 10 mg mL⁻¹. A significant change (a 1.6-fold increase) in the level of the *cox1* gene expression in the root was observed only when exposed to 10 mg mL⁻¹ nnZnO. The expression level of the nuclear genes *AOX1a*,

AOX1d1, and *AOX1d2*, encoding mitochondrial alternative oxidase isoenzymes, was studied. Suppression of *AOX1a* and *AOX1d2* was found in the leaf tissue with all treatments, with the nnZnO having the greatest effect, regardless of the concentration. Transcription of *AOX1d1* under the influence of the studied pollutants (except for 0.3 mg mL⁻¹ blZnO), on the contrary, increased. The greatest growth (by 2.1 times) was observed under the influence of 10 mg mL⁻¹ blZnO. In root tissues, a significant change (increase by 1.8 times) in *AOX1a* transcription occurred only under the action of blZnO at a concentration of 0.3 mg mL⁻¹. An increase in the expression level of the *AOX1d1* and *AOX1d2* genes was found in the roots of all treated seedlings. The exception was *AOX1d1* at a dose of 10 mg mL⁻¹ nnZnO, where a 1.7-fold decrease in activity was noted.

In the leaf tissues, the doses of 2 mg mL⁻¹ and 10 mg mL⁻¹ of the studied pollutants, led to an increase of approximately 36 % in the expression level of the *atp1* gene of the mitochondrial ATPase subunit. At a concentration of 0.3 mg mL⁻¹, blZnO and nnZnO did not affect the number of transcripts of this gene. In comparison to the control group, the analysis of roots showed that all of the treatments significantly inhibited the activity of the *atp1* gene. The largest decrease, almost 3-fold, was recorded under the influence of 10 mg mL⁻¹ blZnO. An analysis of the *nda1* gene expression of an alternative external NADH dehydrogenase in leaf tissues revealed both a decrease of 25 % and 32 % under constant exposure to 10 mg mL⁻¹ blZnO and nnZnO, respectively, and an increase of 21 % and 29 % under the action of 0.3 mg mL⁻¹ nnZnO and 2 mg mL⁻¹ nnZnO, respectively. Regardless of the concentration or size of the ZnO particles, *nda1* activity was shown to be reduced by an average of 53 % in root tissues.

The expression of the *MDH2* gene, whose product NAD-dependent malate dehydrogenase catalyzes the oxidation of malate to

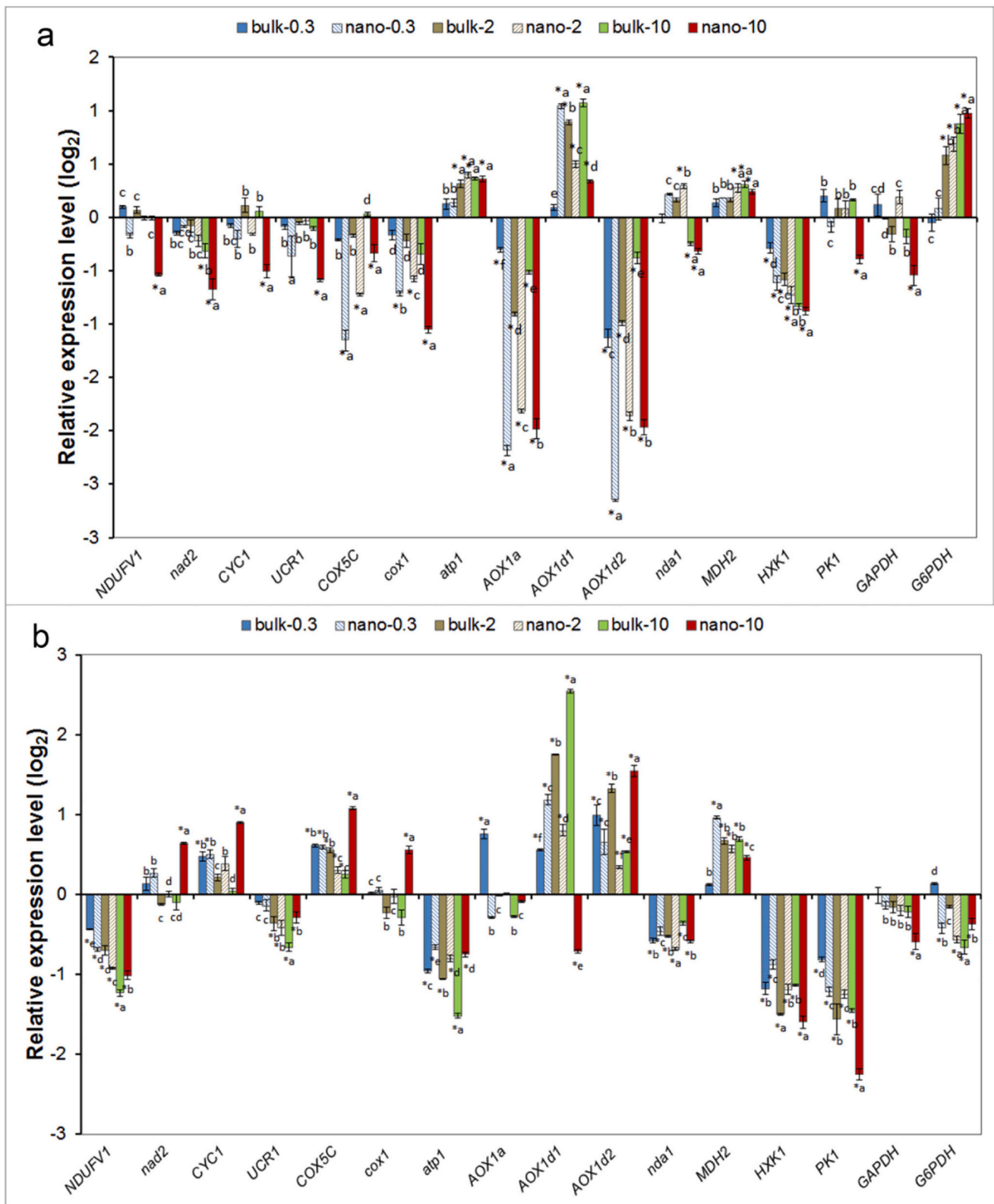


Fig. 10. Variations in the expression levels of respiration-related genes (\log_2 -scale) in (a) leaves and (b) roots of barley under blZnO and nnZnO treatments. *NDUFV1*, NADH dehydrogenase [ubiquinone] flavoprotein 1; *nad2*, NADH dehydrogenase subunit 2; *CYC1*, cytochrome *c1*; *UCR1*, Rieske iron-sulfur protein; *COX5C*, cytochrome *c* oxidase subunit 5; *cox1*, cytochrome *c* oxidase subunit 1; *atp1*, ATPase subunit; *AOX1a*, alternative oxidase 1a; *AOX1d1*, alternative oxidase 1d1; *AOX1d2*, alternative oxidase 1d2; *nda1*, internal alternative NAD(P)H-ubiquinone oxidoreductase; *MDH2*, malate dehydrogenase; *HXK1*, hexokinase; *PK1*, pyruvate kinase; *GAPDH*, glyceraldehyde-3-phosphate dehydrogenase; *G6PDH*, glucose-6-phosphate dehydrogenase. The asterisk indicates the statistical difference from the control. Different letters on the columns refer to statistically significant differences between treatments at $P \leq 0.05$.

oxaloacetate at the last stage of the tricarboxylic acid cycle (TCA) in mitochondria, was studied. A dose of 0.3 mg mL^{-1} blZnO did not cause significant variations in the transcriptional activity of *MDH2* in both leaf and root cells. The other treatments resulted in a nonlinear increase in *MDH2* expression. In the leaves, the increase in *MDH2* levels ranged from 17 % to 31 %. In the treated roots, the excess expression of this gene varied from 46 % to 96 %. Concentrations of 2 mg mL^{-1} and 10 mg mL^{-1} of the studied pollutants led to a rise in transcriptional activity in leaf cells of the glucose-6-phosphate dehydrogenase (*G6PDH*) gene of the pentose phosphate metabolic pathway of plants. In the roots, the doses of 0.3 mg mL^{-1} and 2 mg mL^{-1} blZnO did not affect the activity of *G6PDH*, while other treatments significantly reduced the expression of this gene. The study revealed that the *HXK1*, *GAPDH*, and *PK1* expression levels of these genes encoding the glycolytic enzymes hexokinase, glyceraldehyde-3-phosphate dehydrogenase, and pyruvate kinase demonstrated suppression of *HXK1* transcription in leaf tissue in all variants. The greatest suppression was registered under the action of nnZnO at a concentration of 10 mg mL^{-1} . A decrease in *GAPDH* and *PK1* activity in leaf tissues was noted only under the influence of 10 mg mL^{-1} nnZnO. In root cells, the expression of the *HXK1* and *PK1* genes was reduced compared to the control with all treatments. The greatest decrease (by 3–4 times) was shown when exposed to nnZnO at a concentration of 10 mg mL^{-1} .

4. Discussion

Due to their central position in respiration, nutrition, and biosynthesis, mitochondria can play a vital role in the response of a plant cell under abiotic stress conditions (Dourmap et al., 2020). An analysis of the respiration efficiency in the tissues of the treated barley seedlings revealed, in general, a decrease in a dose-dependent manner under the influence of blZnO and nnZnO in medium (2 mg mL^{-1}) and high (10 mg mL^{-1}) concentrations. The sensitivity of the mitochondrial electron transport chain to the studied compounds depended on the plant organ and ZnO form, and it was higher in root tissues when exposed to a nanosized pollutant. These data are consistent with the results of a zinc content and biomass analysis of the leaf and root tissues of treated barley. This study also showed a significant accumulation of zinc in the mitochondria of leaf and root tissues compared to the control. However, the dependence of the zinc content in the mitochondria on the concentration of introduced metal oxides was not revealed. This may indicate that, unlike chloroplasts (Azarin et al., 2023), mitochondria control the movement of zinc between the organelle and other cellular compartments more effectively, even under conditions of excessive metal exposure. On the other hand, the observed dose-dependent changes in the physiological indices and expression of genes involved in respiration are not associated with the direct accumulation of zinc in mitochondria, but are mediated by the effect of the metal on the cell as a whole (Fig. S1). Higher accumulation of zinc in plant tissues under the influence of nnZnO compared to blZnO has also been previously demonstrated (Vafaie Moghadam et al., 2022; Mirakhorli et al., 2021; Pejman et al., 2021). The high bioaccumulation of nanoparticles is associated with their greater ability for uptake and translocation into plant tissues (Tombuloglu et al., 2019b, 2024). Thus, under the influence of blZnO and nnZnO, a dose-dependent alteration of the mitochondrial fine structure occurred. At low concentrations (0.3 mg mL^{-1}) of the pollutants, the inner membranes showed higher values of indicators than in the control. However, the increase in the membrane apparatus was compensated by a decline in the average size of the mitochondria. The indices of the number of mitochondria per cell, the area of mitochondria, the ratio of the contour length of the inner membrane to the outer one, and the coefficient of energetic efficiency of the mitochondria showed a gradual decrease with an increase in the concentration of the introduced blZnO and nnZnO.

The system of oxidative phosphorylation in mitochondria consists of five multi-subunit protein complexes, which are oxidoreductases

(Complexes I–IV) that form the respiratory chain (ETC) and ATPase (Complex V). It has been established that nnZnO is able to significantly modulate the transcriptome by altering the expression levels of transcription factors, epigenetic regulation genes, and microRNAs (Vafaie Moghadam et al., 2022; Niazi et al., 2023). An analysis of the expressions of subunits of Complex I, Complex III, and Complex IV showed their disruption mainly under the influence of a high concentration of nnZnO. A significant correlation was shown between genes encoding subunits of the same complex (Fig. S1). Moreover, in the root tissues, 10 mg mL^{-1} nnZnO significantly induced the expression of some genes of these complexes, which may indicate attempts to compensate at the transcriptional level for the dramatic decrease in overall respiratory efficiency. At the same time, while a slight increase in the *atp1* gene expression of the ATPase subunit was observed in the leaf tissue in response to medium and high concentrations of pollutants, in the root tissues, the level of *atp1* mRNA significantly decreased in all treatments. There was also a serious decline in the ATP content in the root tissues. In leaves, the ATP content decreased only under the influence of high doses of pollutants, but in this case, alterations in the photosynthetic apparatus also contributed to the total ATP pool (Azarin et al., 2023). Previously, it was also shown that the genes encoding the oxidase subunits of the main ETC pathway are not very sensitive to many stressors (Millar et al., 2011), whereas ATPase is critical for energy metabolism and serves as an indicator of mitochondrial activity (Sabar et al., 2003; Wang et al., 2018).

In addition to the main transporters in the ETC of plant mitochondria, there are shunts represented by alternative oxidase (AOX) and type II NAD(P)H dehydrogenase (ND). The alternative way of respiration does not lead to ATP synthesis and is activated under stressful influences that disrupt the work of the main mitochondrial ETC. An increase in AOX activity under the influence of both heavy metals and other stressors was reported in several studies (Pádua et al., 1999; Dutilleul et al., 2003; Castro-Guerrero et al., 2008; Matecka et al., 2009; Prado et al., 2010; Li and Xing, 2011; Giraud et al., 2008). An interesting result of this study is that the alteration in the transcription of various AOX isoenzymes under the influence of zinc stress was not the same. Thus, in the leaf tissue, the genes encoding the AOX1a and AOX1d2 isoforms were suppressed (especially under the influence of nnZnO), and the *AOX1d1* gene was activated. In root tissues, overexpression of the genes of two isoforms, AOX1d1 and AOX1d2, was observed, while the number of AOX1a transcripts did not generally change. Previously, the co-regulation of AOX and alternative ND for the formation of a shortened respiratory pathway was assumed (Keunen et al., 2011; Clifton et al., 2005). A study on the mRNA level of ND under the action of zinc did not reveal such patterns.

Complexes I and III of mitochondria are the core ROS producers in cells due mainly to electron leakage (Choudhury et al., 2017). In this regard, it was believed that the respiration shunts under stress, in addition to maintaining the functioning of mitochondria by preventing ETC hyperreduction, also contributes to a decrease in ROS production and the prevention of oxidative stress (Suzuki et al., 2012). These results are consistent with the results of the total ROS examination in leaves, where, under the influence of pollutants (with the exception of 10 mg mL^{-1} nnZnO), ROS levels decreased against the background of *AOX1d1* overexpression. However, in root tissues, where the stress factor pressure is higher, a substantial rise in ROS production rate has been reported. This indicates that AOX overexpression cannot always reduce the ROS level. Moreover, increased ROS levels can cause the inhibition of alternative respiration (Wang et al., 2018), thereby leading, in turn, to even greater destabilization and ROS generation. Activation of the antioxidant system components has also been previously demonstrated under the influence of ZnO nanoparticles on *Datura stramonium* and *Glycine max* (Vafaie Moghadam et al., 2022; Mirakhorli et al., 2021), NiFe₂O₄ nanoparticles on *Hordeum vulgare* (Tombuloglu et al., 2019c), TiO₂ nanoparticles on *Helianthus annuus* (Ramadan et al., 2022), CuO nanoparticles on *Triticum aestivum* (Huang et al., 2022),

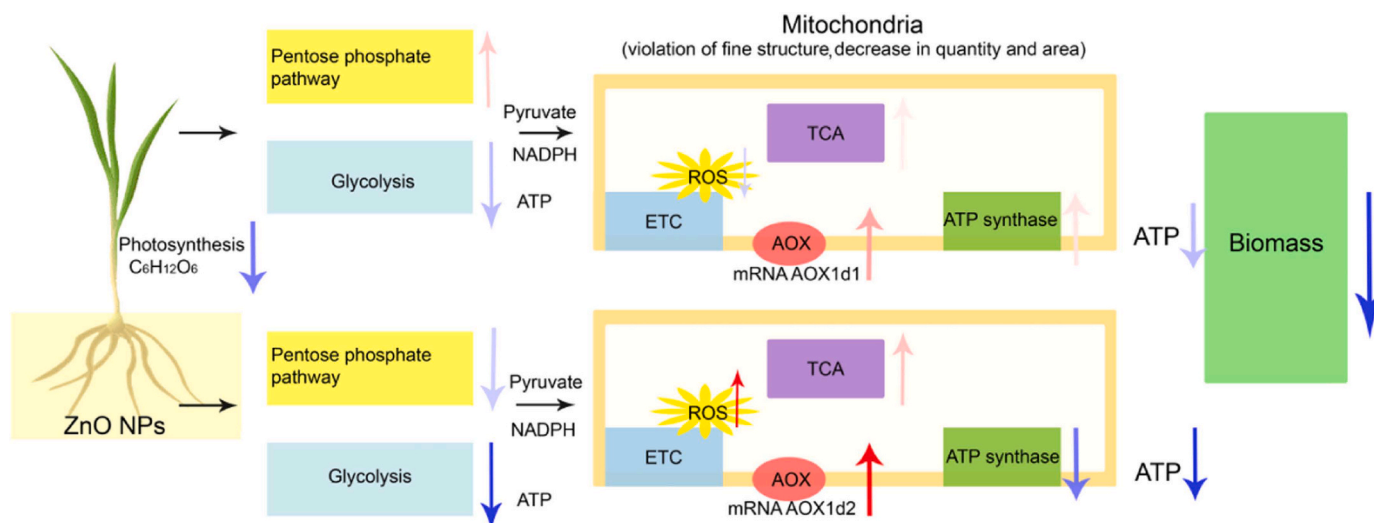


Fig. 11. Schematic illustration of the plausible effects of zinc oxide nanoparticles on *Hordeum vulgare* L. cellular respiration efficiency.

among others. Under oxidative stress in plants, the suppression of TCA cycle and glycolysis, and the activation of the oxidative pentose phosphate pathway, are often noted (Baxter et al., 2007; Lehmann et al., 2012; Chen and Hoehenwarter, 2015; Sipari et al., 2020; Savchenko and Tikhonov, 2021). On the other hand, the protective role of the TCA metabolites in oxidative stress is also suggested (Huang et al., 2016; Du et al., 2017; Awasthi et al., 2019). An analysis of the malate dehydrogenase gene expression, which performs the main part of the metabolic control of the TCA cycle (Zhang and Fernie, 2018; Planchon et al., 2017), revealed its increase in leaf tissues and, to a greater extent, root tissues under the action of blZnO and nnZnO. Metabolic pathway activation of the TCA cycle in plants was also shown under the influence of Al (Awasthi et al., 2019), Ag nanoparticles (Ke et al., 2018), TiO₂ nanoparticles (Wu et al., 2017), and Cu and Fe nanoparticles (Yasmeen et al., 2017). Wu et al. (2017) suggested that a rise in TCA cycle intermediates enabled the provision of important biomolecules damaged by stress. Indeed, TCA cycle intermediates act as substrates for many biological pathways that support a variety of biological functions (Zhang and Fernie, 2018). Organic acids, such as oxalate, malate as well as citrate formed in TCA cycle, were proposed as the main cellular metabolite of heavy metals involved in their transport and vacuolar sequestration (Rausser, 1999; Haydon and Cobbett, 2007; Zhu et al., 2011; Singh and Chauhan, 2011). At the same time, an increase in energy metabolism to resist stress leads to inadequate accessibility of energy for the growth and progression of plants. A significant drop in the biomass of barley was previously revealed under the influence of nnZnO (Azarin et al., 2022). Interestingly, MDH is not a redox-regulated enzyme, and ATP has the greatest inhibitory effect on it (Yoshida and Hisabori, 2016), with ATP levels being reduced during zinc stress.

Cytosolic glycolysis can provide plant adaptation to stress due to an additional source of ATP, which imparts certain metabolic flexibility (Plaxton, 1996). On the other hand, a decrease in carbohydrate metabolism and, ultimately, glucose negatively affects the activity of glycolytic enzymes. Previously studies have shown that toxic doses of nnZnO downregulated the NAM and SUT genes encoding a transcription factor and a sucrose transporter, respectively (Niazi et al., 2023). Moreover, under stress, glycolysis is often replaced by an alternative pentose phosphate pathway, which contributes to less storage of pyruvate as well as ethanol, which are poisonous to the plant (Castillo-González et al., 2018). Ethanol formation mostly occurs in the meristematic cells of the root under the action of aldehyde dehydrogenase, which increases its activity with an excess of zinc (Pardos, 2004). Presumably, this is the reason for the more significant decrease in the transcript number of the glycolytic enzymes hexokinase and pyruvate kinase in roots as

compared to leaves under zinc stress. It has also been shown that glycolytic enzymes function as complexes on the mitochondrial surface, and the stimulation or inhibition of glycolytic enzymes is associated with an increase or inhibition of respiration (Dumont and Rivoal, 2019). The interaction of TCA, glycolysis, and the pentose phosphate pathway as a substitute pathway for glucose oxidation is finely regulated under abiotic stress (Bandehagh and Taylor, 2020). It was assumed that the pentose phosphate pathway, being a metabolic sensor of oxidative stress, controls the quick response to the influence of abiotic factors (Dal Santo et al., 2012; Krüger et al., 2011; Cardi et al., 2011). The core monitoring enzyme of this pathway is glucose-6-phosphate dehydrogenase (G6PDH) (Esposito, 2016). Increased activity and expression of G6PDH were demonstrated when plants were exposed to salt stress (Wang et al., 2008; Nemoto and Sasakuma, 2000; Yang et al., 2014) and drought (Landi et al., 2016). A change in the G6PDH level was also detected when plants were exposed to cadmium and arsenic (Devi et al., 2007; Pérez-Chaca et al., 2014; Xu et al., 2003; Corpas et al., 2016). In this study, a rise in the level of G6PDH transcripts was reported in leaf tissue in accordance with medium and high concentrations of blZnO and nnZnO. Conversely, in root tissues, the studied zinc compounds, especially in the nanosized form, caused a reduction in G6PDH expression. In this case, a high concentration of nnZnO caused severe stress on root cells that mediated a decrease in the pentose phosphate pathway and glycolysis, presumably by a significant drop in carbohydrate metabolism, which is usually detected when exposed to various stressors (Wu et al., 2017). In general, by increasing the activity of ATPase, AOX, TCA, and the pentose phosphate pathway, plants compensated for the effect of low doses of the pollutants on energy metabolism. This was especially noticeable in the leaves, and was reflected in the nonlinear change in a number of integral respiratory-related indices. At maximum exposure, the transcription of genes for oxidative phosphorylation, glycolysis, the pentose phosphate pathway, and external NADH dehydrogenase was reduced, which in turn led to an increase in ROS and a decrease in respiratory efficiency, mitochondrial energy efficiency, and ATP. As a result, it was expressed in a significant decrease in plant biomass.

5. Conclusion

There was a concentration-dependent and size-dependent (bulk or nano) disruption of energy processes in barley seedlings when exposed to blZnO and nnZnO. The more pronounced effects of nnZnO compared to blZnO were likely due to its greater bioavailability to plants, as confirmed by the data on zinc accumulation in tissues. In general, a significant rearrangement of the transcription of the genes of oxidative

phosphorylation, glycolysis, the oxidative pentose phosphate pathway, AOX and the TCA cycle was shown (Fig. 11). The changes in transcriptional activity compensated to some extent for the effects of blZnO and nnZnO at low doses. However, high doses of the pollutants (especially nnZnO) led to a reduction in respiratory efficiency, a decrease in ATP synthesis and an increase in ROS production, which indicated the disorganization of oxidative phosphorylation. This research is important for understanding and predicting the impacts of nanoparticles on plants and the environment.

CRedit authorship contribution statement

Andrey Plotnikov: Writing – review & editing, Software. **Saglara Mandzhieva:** Writing – review & editing, Software, Investigation. **Rahul Kumar:** Writing – review & editing, Visualization. **Jean Wan Hong Yong:** Writing – review & editing, Visualization, Funding acquisition, Conceptualization. **Tatiana Minkina:** Writing – review & editing, Validation, Resources, Investigation. **Nadezhda Duplii:** Software, Methodology, Formal analysis. **Aleksei Fedorenko:** Visualization, Software, Formal analysis. **Shafaque Sehar:** Writing – review & editing, Software, Conceptualization. **Vishnu D. Rajput:** Writing – review & editing, Supervision, Resources, Project administration, Funding acquisition, Conceptualization. **Kirill Azarin:** Writing – original draft, Methodology, Formal analysis, Data curation. **Alexander Usatov:** Writing – original draft, Methodology, Formal analysis, Data curation.

Declaration of Competing Interest

The authors declare that they have no known competing financial interests or personal relationships that could have appeared to influence the work reported in this paper.

Data availability

Data will be made available on request.

Acknowledgements

The Russian Federation's Ministry of Science and Higher Education (no. FENW-2023-0008). provided funding for this study.

Appendix A. Supporting information

Supplementary data associated with this article can be found in the online version at [doi:10.1016/j.ecoenv.2024.116670](https://doi.org/10.1016/j.ecoenv.2024.116670).

References

- Abdelgawad, H., Hassan, Y.M., Alotaibi, M.O., Mohammed, A.E., Saleh, A.M., 2020. C3 and C4 plant systems respond differently to the concurrent challenges of mercuric oxide nanoparticles and future climate CO₂. *Sci. Total Environ.* 749, 142356 <https://doi.org/10.1016/j.scitotenv.2020.142356>.
- Adil, M.F., Sehar, S., Ma, Z.X., Tahira, K., Askri, S.M.H., El-Sheikh, M.A., Aqeel, A., Zhou, F.R., Zhao, P., Shamsi, I.H., 2024. Insights into the alleviation of cadmium toxicity in rice by nano-zinc and *Serendipita indica*: Modulation of stress-responsive gene expression and antioxidant defense system activation. *Environ. Pollut.* 350, 123952. <https://doi.org/10.1016/j.envpol.2024.123952>.
- Ahmed, B., Dwivedi, S., Abdin, M.Z., Azam, A., Al-Shaeri, M., Khan, M.S., Saquib, Q., Al-Khedhairy, A.A., Musarrat, J., 2017. Mitochondrial and chromosomal damage induced by oxidative stress in Zn²⁺ ions, ZnO-bulk and ZnO-NPs treated *Allium cepa* roots. *Sci. Rep.* 7, 40685 <https://doi.org/10.1038/srep40685>.
- Ahmed, B., Syed, A., Rizvi, A., Shahid, M., Bahkali, A.H., Khan, M.S., Musarrat, J., 2021. Impact of metal-oxide nanoparticles on growth, physiology and yield of tomato (*Solanum lycopersicum* L.) modulated by *Azotobacter salinestrans* strain ASM. *Environ. Pollut.* 269, 116218 <https://doi.org/10.1016/j.envpol.2020.116218>.
- Al-Amri, N., Tombuloglu, H., Slimani, Y., Akhtar, S., Barghouthi, M., Almessiere, M., Alshammari, T., Baykal, A., Sabit, H., Ercan, I., Ozcelik, S., 2020. Size effect of iron (III) oxide nanomaterials on the growth, and their uptake and translocation in common wheat (*Triticum aestivum* L.). *Ecotoxicol. Environ. Saf.* 194, 110377 <https://doi.org/10.1016/j.ecoenv.2020.110377>.

- Alhailthoul, H.A.A., Ali, B., Alghanem, S.M.S., Zulfiqar, F., Al-Robai, S.A., Ercisli, S., Yong, J.W.H., Moosa, A., Irfan, E., Ali, Q., Irshad, M.A., Abeer, A.H.A., 2023. Effect of green-synthesized copper oxide nanoparticles on growth, physiology, nutrient uptake, and cadmium accumulation in *Triticum aestivum* (L.). *Ecotoxicology and Environmental Safety* 268, 115701. <https://doi.org/10.1016/j.ecoenv.2023.115701>.
- Awasthi, J.P., Saha, B., Panigrahi, J., Yanase, E., Koyama, H., Panda, S.K., 2019. Redox balance, metabolic fingerprint and physiological characterization in contrasting North East Indian rice for Aluminum stress tolerance. *Sci. Rep.* 9, 8681. <https://doi.org/10.1038/s41598-019-45158-3>.
- Azarin, K., Usatov, A., Makarenko, M., Kozel, N., Kovalevich, A., Dremuk, I., Yemelyanova, A., Logacheva, M., Fedorenko, A., Averina, N., 2020. A point mutation in the photosystem I P700 chlorophyll a apoprotein A1 gene confers variegation in *Helianthus annuus* L. *Plant Mol. Biol.* 103, 373–389. <https://doi.org/10.1007/s11103-020-00997-x>.
- Azarin, K., Usatov, A., Minkina, T., Plotnikov, A., Kasyanova, A., Fedorenko, A., Duplii, N., Vechkanov, E., Rajput, V.D., Mandzhieva, S., Alamri, S., 2022. Effects of ZnO nanoparticles and its bulk form on growth, antioxidant defense system and expression of oxidative stress related genes in *Hordeum vulgare* L. *Chemosphere* 287, 132167. <https://doi.org/10.1016/j.chemosphere.2021.132167>.
- Azarin, K., Usatov, A., Minkina, T., Duplii, N., Kasyanova, A., Fedorenko, A., Khachumov, V., Mandzhieva, S., Rajput, V.D., 2023. Effects of bulk and nano-ZnO particles on functioning of photosynthetic apparatus in barley (*Hordeum vulgare* L.). *Environ. Res.* 216, 114748 <https://doi.org/10.1016/j.envres.2022.114748>.
- Bandehagh, A., Taylor, N.L., 2020. Can alternative metabolic pathways and shunts overcome salinity induced inhibition of central carbon metabolism in crops? *Front. Plant Sci.* 11, 1072. <https://doi.org/10.3389/fpls.2020.01072>.
- Barhoum, A., Rastogi, V.K., Mahur, B.K., Rastogi, A., Abdel-Haleem, F.M., Samyn, P., 2022. Nanocelluloses as new generation materials: natural resources, structure related properties, engineering nanostructures, and technical challenges. *Mater. Today Chem.* 26, 101247. <https://doi.org/10.1016/j.mtchem.2022.101247>.
- Baskar, V., Safia, N., Sree Preethy, K., Dhivya, S., Thiruvengadam, M., Sathishkumar, R., 2021. A comparative study of phytotoxic effects of metal oxide (CuO, ZnO and NiO) nanoparticles on *in-vitro* grown *Abelmoschus esculentus*. *Plant Biosyst. Plant Biosyst. - Int. J. Deal. Asp. Plant Biol.* 155, 374–383. <https://doi.org/10.1080/11263504.2020.1753843>.
- Baxter, C.J., Redestig, H., Schauer, N., Reipsilber, D., Patil, K.R., Nielsen, J., Selbig, J., Liu, J., Fernie, A.R., Sweetlove, L.J., 2007. The metabolic response of heterotrophic *Arabidopsis* cells to oxidative stress. *Plant Physiol.* 143, 312–325. <https://doi.org/10.1104/pp.106.090431>.
- Boxall, A., Chaudhry, Q., Cinclair, C., Jones, A., Aitken, R., Jefferson, B., Watts, C., 2007. Current and future predicted environmental exposure to engineered nanoparticles. *central science laboratory, York. Saf. Nanomater. Interdiscip. Res. Cent. Rep.* 1–13.
- Cardi, M., Chibani, K., Cafasso, D., Rouhler, N., Jacquot, J.-P., Esposito, S., 2011. Abscisic acid effects on activity and expression of barley (*Hordeum vulgare*) plastidial glucose-6-phosphate dehydrogenase. *J. Exp. Bot.* 62, 4013–4023. <https://doi.org/10.1093/jxb/err100>.
- Castillo-González, J., Ojeda-Barrios, D., Hernández-Rodríguez, A., González-Franco, A. C., Robles-Hernández, L., López-Ochoa, G.R., 2018. Zinc metalloenzymes in plants. *Interciencia* 43 (4), 242–248.
- Castro-Guerrero, N.A., Rodríguez-Zavala, J.S., Marín-Hernández, A., Rodríguez-Enríquez, S., Moreno-Sánchez, R., 2008. Enhanced alternative oxidase and antioxidant enzymes under Cd²⁺ stress in *Euglena*. *J. Bioenerg. Biomembr.* 40, 227–235. <https://doi.org/10.1007/s10863-007-9098-6>.
- Che, X., Ding, R., Li, Y., Zhang, Z., Gao, H., Wang, W., 2018. Mechanism of long-term toxicity of CuO NPs to microalgae. *Nanotoxicology* 12, 923–939. <https://doi.org/10.1080/17435390.2018.1498928>.
- Chemingui, H., Smiri, M., Missaoui, T., Hafiane, A., 2019. Zinc oxide nanoparticles induced oxidative stress and changes in the photosynthetic apparatus in fenugreek (*Trigonella foenum-graecum* L.). *Bull. Environ. Contam. Toxicol.* 102, 477–485. <https://doi.org/10.1007/s00128-019-02590-5>.
- Chen, J., Dou, R., Yang, Z., You, T., Gao, X., Wang, L., 2018. Phytotoxicity and bioaccumulation of zinc oxide nanoparticles in rice (*Oryza sativa* L.). *Plant Physiol. Biochem.* 130, 604–612. <https://doi.org/10.1016/j.plaphy.2018.08.019>.
- Chen, Y., Hoehenwarter, W., 2015. Changes in the phosphoproteome and metabolome link early signaling events to rearrangement of photosynthesis and central metabolism in salinity and oxidative stress response in *Arabidopsis*. *Plant Physiol.* 169, 3021–3033. <https://doi.org/10.1104/pp.15.01486>.
- Chomczynski, P., Sacchi, N., 1987. Single-step method of RNA isolation by acid guanidinium thiocyanate-phenol-chloroform extraction. *Anal. Biochem.* 162, 156–159. [https://doi.org/10.1016/0003-2697\(87\)90021-2](https://doi.org/10.1016/0003-2697(87)90021-2).
- Choudhury, F.K., Rivero, R.M., Blumwald, E., Mittler, R., 2017. Reactive oxygen species, abiotic stress and stress combination. *Plant J.* 90, 856–867. <https://doi.org/10.1111/taj.13299>.
- Clifton, R., Lister, R., Parker, K.L., Sappl, P.G., Elhafez, D., Millar, A.H., Day, D.A., Whelan, J., 2005. Stress-induced co-expression of alternative respiratory chain components in *Arabidopsis thaliana*. *Plant Mol. Biol.* 58, 193. <https://doi.org/10.1007/s11103-005-5514-7>.
- Corpas, F.J., Aguayo-Trinidad, S., Ogawa, T., Yoshimura, K., Shigeoka, S., 2016. Activation of NADPH-recycling systems in leaves and roots of *Arabidopsis thaliana* under arsenic-induced stress conditions is accelerated by knock-out of Nudix hydrolase 19 (*AtNUDX19*) gene. *J. Plant Physiol.* 192, 81–89. <https://doi.org/10.1016/j.jplph.2016.01.010>.
- Dai, Y., Wang, Z., Zhao, J., Xu, Lili, Xu, Lina, Yu, X., Wei, Y., Xing, B., 2018. Interaction of CuO nanoparticles with plant cells: internalization, oxidative stress, electron

- transport chain disruption, and toxicogenomic responses. *Environ. Sci.: Nano* 5, 2269–2281. <https://doi.org/10.1039/C8EN00222C>.
- Dal Santo, S., Stampfl, H., Krassensky, J., Kempa, S., Gibon, Y., Petutschnig, E., Rozhon, W., Heuck, A., Clausen, T., Jonak, C., 2012. Stress-Induced gsk3 regulates the redox stress response by phosphorylating glucose-6-phosphate dehydrogenase in *Arabidopsis*. *Plant Cell* 24, 3380–3392. <https://doi.org/10.1105/tpc.112.101279>.
- Devi, R., Munjral, N., Gupta, A.K., Kaur, N., 2007. Cadmium induced changes in carbohydrate status and enzymes of carbohydrate metabolism, glycolysis and pentose phosphate pathway in pea. *Environ. Exp. Bot.* 61, 167–174. <https://doi.org/10.1016/j.envexpbot.2007.05.006>.
- Dourmap, C., Roque, S., Morin, A., Caubrière, D., Kerdiles, M., Béguin, K., Perdoux, R., Reynoud, N., Bourdet, L., Audebert, P.-A., Moullec, J.L., Couée, I., 2020. Stress signalling dynamics of the mitochondrial electron transport chain and oxidative phosphorylation system in higher plants. *Ann. Bot.* 125, 721–736. <https://doi.org/10.1093/aob/mcz184>.
- Du, C., Zhang, B., He, Y., Hu, C., Ng, Q.X., Zhang, H., Ong, C.N., Lin, Z., 2017. Biological effect of aqueous C60 aggregates on *Scenedesmus obliquus* revealed by transcriptomics and non-targeted metabolomics. *J. Hazard. Mater.* 324, 221–229. <https://doi.org/10.1016/j.jhazmat.2016.10.052>.
- Dumont, S., Rivoal, J., 2019. Consequences of oxidative stress on plant glycolytic and respiratory metabolism. *Front. Plant Sci.* 10, 166. <https://doi.org/10.3389/fpls.2019.00166>.
- Dutilleul, C., Garmier, M., Noctor, G., Mathieu, C., Chétrit, P., Foyer, C.H., De Paepe, R., 2003. Leaf mitochondria modulate whole cell redox homeostasis, set antioxidant capacity, and determine stress resistance through altered signaling and diurnal regulation. *Plant Cell* 15, 1212–1226. <https://doi.org/10.1105/tpc.009464>.
- Elmer, W., White, J.C., 2018. The future of nanotechnology in plant pathology. *Annual Review of Phytopathology* 58, 111–133. <https://doi.org/10.1146/annurev-phyto-080417-050108>.
- Elsheery, N.I., Sunoj, V.S.J., Wen, Y., Zhu, J.J., Muralidharan, G., Cao, K.F., 2020. Foliar application of nanoparticles mitigates the chilling effect on photosynthesis and photoprotection in sugarcane. *Plant Physiol. Biochem.* 149, 50–60. <https://doi.org/10.1016/j.plaphy.2020.01.035>.
- Esposito, S., 2016. Nitrogen assimilation, abiotic stress and glucose 6-phosphate dehydrogenase: the full circle of reductants. *Plants* 5, 24. <https://doi.org/10.3390/plants5020024>.
- Faisal, M., Saquib, Q., Alatar, A.A., Al-Khedhairi, A.A., Ahmed, M., Ansari, S.M., Alwathnani, H.A., Dwivedi, S., Musarrat, J., Praveen, S., 2016. Cobalt oxide nanoparticles aggravate DNA damage and cell death in eggplant via mitochondrial swelling and NO signaling pathway. *Biol. Res.* 49, 20. <https://doi.org/10.1186/s40659-016-0080-9>.
- Fincheira, P., Tortella, G., Seabra, A.B., Quiroz, A., Diez, M.C., Rubilar, O., 2021. Nanotechnology advances for sustainable agriculture: current knowledge and prospects in plant growth modulation and nutrition. *Planta* 254, 1–25. <https://doi.org/10.1007/s00425-021-03714-0>.
- Giraud, E., Ho, L.H.M., Clifton, R., Carroll, A., Estavillo, G., Tan, Y.-F., Howell, K.A., Ivanova, A., Pogson, B.J., Millar, A.H., Whelan, J., 2008. The absence of ALTERNATIVE OXIDASE1a in *Arabidopsis* results in acute sensitivity to combined light and drought stress. *Plant Physiol.* 147, 595–610. <https://doi.org/10.1104/pp.107.115121>.
- Gottschalk, F., Sonderer, T., Scholz, R.W., Nowack, B., 2009. Modeled environmental concentrations of engineered nanomaterials (TiO₂, ZnO, Ag, CNT, Fullerenes) for different regions. *Environ. Sci. Technol.* 43, 9216–9222. <https://doi.org/10.1021/es9015553>.
- Haider, F.U., Zulfqar, U., ul Ain, N., Hussain, S., Maqsood, M.S., Ejaz, M., Yong, J.W.H., Li, Y., 2024. Harnessing plant extracts for eco-friendly synthesis of iron nanoparticle (Fe-NPs): Characterization and their potential applications for ameliorating environmental pollutants. *Ecotoxicology and Environmental Safety* 281, 116620. <https://doi.org/10.1016/j.ecoenv.2024.116620>.
- Hanif, M., Munir, N., Abideen, Z., Yong, J.W.H., El-Keblawy, A., El-Sheikh, M.A., 2024. Synthesis and optimization of nanoparticles from *Phragmites karka* for improves tomato growth and salinity resilience. *Biocatalysis and Agricultural Biotechnology* 55, 102972. <https://doi.org/10.1016/j.bcab.2023.102972>.
- Hayat, S., Pichtel, J., Faizan, M., Fariduddin, Q. (Eds.), 2020. Sustainable agriculture reviews 41: nanotechnology for plant growth and development, sustainable agriculture reviews. Springer international publishing, Cham. <https://doi.org/10.1007/978-3-030-33996-8>.
- Haydon, M.J., Cobbett, C.S., 2007. Transporters of ligands for essential metal ions in plants. *N. Phytol.* 174, 499–506. <https://doi.org/10.1111/j.1469-8137.2007.02051.x>.
- Huang, H., Jian, Q., Jiang, Y., Duan, X., Qu, H., 2016. Enhanced chilling tolerance of banana fruit treated with malic acid prior to low-temperature storage. *Postharvest Post. Biol. Technol.* 111, 209–213. <https://doi.org/10.1016/j.postharvbio.2015.09.008>.
- Huang, G., Zuverza-Mena, N., White, J.C., Hu, H., Xing, B., Dhankher, O.P., 2022. Simultaneous exposure of wheat (*Triticum aestivum* L.) to CuO and S nanoparticles alleviates toxicity by reducing Cu accumulation and modulating antioxidant response. *Sci. Total Environ.* 839, 156285 <https://doi.org/10.1016/j.scitotenv.2022.156285>.
- Iftikhar, A., Ali, S., Yasmeen, T., Arif, M.S., Zubair, M., Rizwan, M., Alhailoul, H.A.S., Alayafi, A.A.M., Soliman, M.H., 2019. Effect of gibberellic acid on growth, photosynthesis and antioxidant defense system of wheat under zinc oxide nanoparticle stress. *Environ. Pollut. Environ. Pollut.* 254, 113109 <https://doi.org/10.1016/j.envpol.2019.113109>.
- Iranbakhsh, A., Oraghi Ardebili, Z., Oraghi Ardebili, N., 2021. Synthesis and characterization of zinc oxide nanoparticles and their impact on plants. In: Singh, V., Singh, S., Tripathi, D.K., Prasad, S.M., Chauhan, D.K. (Eds.), *Plant Responses to Nanomaterials*. Springer International Publishing, Cham, pp. 33–93. https://doi.org/10.1007/978-3-030-36740-4_3.
- Jalil, S., Nazir, M.M., Ali, Q., Zulfqar, F., Moosa, A., Altaf, M.A., Zaid, A., Nafees, M.A., Yong, J.W.H., Jin, X., 2023a. Zinc and nano zinc mediated alleviation of heavy metals and metalloids in plants: an overview. *Funct. Plant Biol.* 50, 23021. <https://doi.org/10.1071/FP23021>.
- Jalil, S., Nazir, M. M., Al-Huqail, A. A. Ali, B., Al-Qthanin, R. N., Asad, M.A.U., Eweda, M. A., Zulfqar, F., Onursal, N., Masood, H. A., Yong, J. W. H., Jin, X., 2023b. Silicon nanoparticles alleviate cadmium toxicity in rice by modulating the nutritional profile and triggering stress-responsive genetic mechanisms. *Ecotoxicology and Environmental Safety*, 268, 115699. <https://doi.org/10.1016/j.ecoenv.2023.115699>.
- Jan, N., Majeed, N., Ahmad, M., Ahmad Lone, W., John, R., 2022. Nano-pollution: why it should worry us. *Chemosphere* 302, 134746. <https://doi.org/10.1016/j.chemosphere.2022.134746>.
- Javed, R., Usman, M., Yücesan, B., Zia, M., Gürel, E., 2017. Effect of zinc oxide (ZnO) nanoparticles on physiology and steviol glycosides production in micropropagated shoots of *Stevia rebaudiana* Bertoni. *Plant Physiol. Biochem.* 110, 94–99. <https://doi.org/10.1016/j.plaphy.2016.05.032>.
- Jhanzab, H., Razzaq, A., Bibi, Y., Yasmeen, F., Yamaguchi, H., Hitachi, K., Tsuchida, K., Komatsu, S., 2019. Proteomic analysis of the effect of inorganic and organic chemicals on silver nanoparticles in wheat. *IJMS* 20, 825. <https://doi.org/10.3390/ijms20040825>.
- Kang, M., Liu, Y., Weng, Y., Wang, H., Bai, X., 2023. A critical review on the toxicity regulation and ecological risks of zinc oxide nanoparticles to plants. *Environ. Sci.: Nano*. <https://doi.org/10.1039/D3EN00630A>.
- Ke, M., Qu, Q., Peijnenburg, W.J.G.M., Li, X., Zhang, M., Zhang, Z., Lu, T., Pan, X., Qian, H., 2018. Phytotoxic effects of silver nanoparticles and silver ions to *Arabidopsis thaliana* as revealed by analysis of molecular responses and of metabolic pathways. *Sci. Total Environ.* 644, 1070–1079. <https://doi.org/10.1016/j.scitotenv.2018.07.061>.
- Keunen, E., Remans, T., Bohler, S., Vangronsveld, J., Cuypers, A., 2011. Metal-induced oxidative stress and plant mitochondria. *IJMS* 12, 6894–6918. <https://doi.org/10.3390/ijms12106894>.
- Khan, S., Mansoor, S., Rafi, Z., Kumari, B., Shoaib, A., Saeed, M., et al., 2022. A review on nanotechnology: properties, applications, and mechanistic insights of cellular uptake mechanisms. *J. Mol. Liq.* 348, 118008. <https://doi.org/10.1016/j.molliq.2021.118008>.
- Kozel, N.V., Shalygo, N.V., 2009. Barley leaf antioxidant system under photooxidative stress induced by Rose Bengal. *Russ. J. Plant Physiol.* 56, 316–322. <https://doi.org/10.1134/S1021443709030030>.
- Krüger, A., Grüning, N.-M., Wamelink, M.M.C., Kerick, M., Kirpy, A., Parkhomchuk, D., Bluemel, K., Schweiger, M.-R., Soldatov, A., Lehrach, H., Jakobs, C., Ralsler, M., 2011. The pentose phosphate pathway is a metabolic redox sensor and regulates transcription during the antioxidant response. *Antioxid. Redox Signal* 15, 311–324. <https://doi.org/10.1089/ars.2010.3797>.
- Landi, S., Nurcato, R., De Lillo, A., Lentini, M., Grillo, S., Esposito, S., 2016. Glucose-6-phosphate dehydrogenase plays a central role in the response of tomato (*Solanum lycopersicum*) plants to short and long-term drought. *Plant Physiol. Biochem.* 105, 79–89. <https://doi.org/10.1016/j.plaphy.2016.04.013>.
- Lee, C.W., Mahendra, S., Zodrow, K., Li, D., Tsai, Y., Braam, J., Alvarez, P.J.J., 2010. Developmental phytotoxicity of metal oxide nanoparticles to *Arabidopsis thaliana*. *Environ Toxicol Chem. Environ. Toxic. Chem.* 29, 669–675. <https://doi.org/10.1002/etc.58>.
- Lehmann, M., Laxa, M., Sweetlove, L.J., Fernie, A.R., Obata, T., 2012. Metabolic recovery of *Arabidopsis thaliana* roots following cessation of oxidative stress. *Metabolomics* 8, 143–153. <https://doi.org/10.1007/s11306-011-0296-1>.
- Li, Z., Xing, D., 2011. Mechanistic study of mitochondria-dependent programmed cell death induced by aluminium phytotoxicity using fluorescence techniques. *J. Exp. Bot.* 62, 331–343. <https://doi.org/10.1093/jxb/erq279>.
- Lin, D., Xing, B., 2007. Phytotoxicity of nanoparticles: Inhibition of seed germination and root growth. *Environ. Pollut. Ion.-.* 150, 243–250. <https://doi.org/10.1016/j.envpol.2007.01.016>.
- Lin, D., Xing, B., 2008. Root uptake and phytotoxicity of ZnO nanoparticles. *Environ. Sci. Technol.* 42, 5580–5585. <https://doi.org/10.1021/es800422x>.
- Livak, K.J., Schmittgen, T.D., 2001. Analysis of relative gene expression data using real-time quantitative pcr and the 2^{-ΔΔC_T} method. *Methods* 25, 402–408. <https://doi.org/10.1006/meth.2001.1262>.
- López-Moreno, M.L., De La Rosa, G., Hernández-Viezas, J.Á., Castillo-Michel, H., Botez, C.E., Peralta-Video, J.R., Gardea-Torresdes, J.L., 2010. Evidence of the differential biotransformation and genotoxicity of ZnO and CeO₂ nanoparticles on soybean (*Glycine max*) Plants. *Environ. Sci. Technol.* 44, 7315–7320. <https://doi.org/10.1021/es903891g>.
- Lysenko, E.A., Klaus, A.A., Kartashov, A.V., Kusnetsov, V.V., 2019. Distribution of Cd and other cations between the stroma and thylakoids: a quantitative approach to the search for Cd targets in chloroplasts. *Photosynth. Res.* 139, 337–358. <https://doi.org/10.1007/s11120-018-0528-6>.
- Malecka, A., Derba-Maceluch, M., Kaczorowska, K., Piechalak, A., Tomaszewska, B., 2009. Reactive oxygen species production and antioxidative defense system in pea root tissues treated with lead ions: mitochondrial and peroxisomal level. *Acta Physiol. Plant* 31, 1065–1075. <https://doi.org/10.1007/s11738-009-0327-y>.
- Marmiroli, M., Mussi, F., Pagano, L., Imperiale, D., Lencioni, G., Villani, M., Zappettini, A., White, J.C., Marmiroli, N., 2020. Cadmium sulfide quantum dots impact *Arabidopsis thaliana* physiology and morphology. *Chemosphere* 240, 124856. <https://doi.org/10.1016/j.chemosphere.2019.124856>.

- Millar, A.H., Whelan, J., Soole, K.L., Day, D.A., 2011. Organization and regulation of mitochondrial respiration in plants. *Annu. Rev. Plant Biol.* 62, 79–104. <https://doi.org/10.1146/annurev-arplant-042110-103857>.
- Minkina, T.M., Fedorov, Yu.A., Nevidomskaya, D.G., Pol'shina, T.N., Mandzhieva, S.S., Chaplygin, V.A., 2017. Heavy metals in soils and plants of the Don river estuary and the Taganrog Bay coast. *Eurasia Soil Sc.* 50, 1033–1047. <https://doi.org/10.1134/S1064229317070067>.
- Mirakhorli, T., Ardebili, Z.O., Ladan-Moghadam, A., Danaee, E., 2021. Bulk and nanoparticles of zinc oxide exerted their beneficial effects by conferring modifications in transcription factors, histone deacetylase, carbon and nitrogen assimilation, antioxidant biomarkers, and secondary metabolism in soybean. *PLoS One* 16, e0256905. <https://doi.org/10.1371/journal.pone.0256905>.
- Molnár, Á., Papp, M., Zoltán Kovács, D., Béltéky, P., Oláh, D., Feigl, G., Szöllösi, R., Rázga, Z., Ördög, A., Erdei, L., Rónavári, A., Kónya, Z., Kolbert, Z., 2020. Nitro-oxidative signalling induced by chemically synthesized zinc oxide nanoparticles (ZnO NPs) in *Brassica* species. *Chemosphere* 251, 126419. <https://doi.org/10.1016/j.chemosphere.2020.126419>.
- Nair, P.M.G., Chung, I.M., 2017. Regulation of morphological, molecular and nutrient status in *Arabidopsis thaliana* seedlings in response to ZnO nanoparticles and Zn ion exposure. *Sci. Total Environ.* 575, 187–198. <https://doi.org/10.1016/j.scitotenv.2016.10.017>.
- Nam, N.H., Luong, N.H., 2019. Nanoparticles: synthesis and applications. *Materials for Biomedical Engineering*, 211–240. <https://doi.org/10.1016/b978-0-08-102814-8.00008-1>, 2019.
- Nemoto, Y., Sasakuma, T., 2000. Specific expression of glucose-6-phosphate dehydrogenase (*G6PDH*) gene by salt stress in wheat (*Triticum aestivum* L.). *Plant Sci.* 158, 53–60. [https://doi.org/10.1016/S0168-9452\(00\)00305-8](https://doi.org/10.1016/S0168-9452(00)00305-8).
- Niazi, A., Iranbakhsh, A., Esmael Zadeh, M., Ebad, M., Oraghi Ardebili, Z., 2023. Zinc oxide nanoparticles (ZnONPs) influenced seed development, grain quality, and remobilization by affecting the transcription of microRNA 171 (miR171), miR156, *NAM*, and *SUT* genes in wheat (*Triticum aestivum*): a biological advantage and risk assessment study. *Protoplasma* 260, 839–851. <https://doi.org/10.1007/s00709-022-01817-3>.
- Pádua, M., Aubert, S., Casimiro, A., Bligny, R., Millar, A.H., Day, D.A., 1999. Induction of alternative oxidase by excess copper in sycamore cell suspensions. *Plant Physiol. Biochem.* 37, 131–137. [https://doi.org/10.1016/S0981-9428\(99\)80074-6](https://doi.org/10.1016/S0981-9428(99)80074-6).
- Pang, S., Zhao, L., An, Y., 2024. Advanced developments in nanotechnology and nanomaterials for the oil and gas industry: A review. *Geoenvironment Science and Engineering* 238, 212872. <https://doi.org/10.1016/j.geoen.2024.212872>.
- Pardos, J.A., 2004. Respuestas de las plantas al anegamiento del suelo. *For. Syst.* 13 (4), 101–107.
- Paukov, V.S., Kazanskaya, T.A., Frolov, V.A., 1971. Quantitative analysis of some components of myocardial electron micrographs. *Bull. Exp. Biol. Med.* 71, 469–472. <https://doi.org/10.1007/BF00808503>.
- Pejam, F., Ardebili, Z.O., Ladan-Moghadam, A., Danaee, E., 2021. Zinc oxide nanoparticles mediated substantial physiological and molecular changes in tomato. *PLoS One* 16, e0248778. <https://doi.org/10.1371/journal.pone.0248778>.
- Pérez-Chaca, M.V., Rodríguez-Serrano, M., Molina, A.S., Pedranzani, H.E., Zirulnik, F., Sandalo, L.M., Romero-Puertas, M.C., 2014. Cadmium induces two waves of reactive oxygen species in *Glycine max* (L.) roots. *Plant Cell Environ.* 37, 1672–1687. <https://doi.org/10.1111/pce.12280>.
- Piccinno, F., Gottschalk, F., Seeger, S., Nowack, B., 2012. Industrial production quantities and uses of ten engineered nanomaterials in Europe and the world. *J. Nanopart. Res.* 14, 1109. <https://doi.org/10.1007/s11051-012-1109-9>.
- Planchon, M., Léger, T., Spalla, O., Huber, G., Ferrari, R., 2017. Metabolomic and proteomic investigations of impacts of titanium dioxide nanoparticles on *Escherichia coli*. *PLoS ONE* 12, e0178437. <https://doi.org/10.1371/journal.pone.0178437>.
- Plaxton, W.C., 1996. The organization and regulation of plant glycolysis. *Annu. Rev. Plant Physiol. Plant. Mol. Biol.* 47, 185–214. <https://doi.org/10.1146/annurev-arplant.47.1.185>.
- Prado, C., Rodríguez-Montelongo, L., González, J.A., Pagano, E.A., Hilal, M., Prado, F.E., 2010. Uptake of chromium by *Salvinia minima*: Effect on plant growth, leaf respiration and carbohydrate metabolism. *J. Hazard. Mater.* 177, 546–553. <https://doi.org/10.1016/j.jhazmat.2009.12.067>.
- Rai-Kalal, P., Jajoo, A., 2021. Priming with zinc oxide nanoparticles improve germination and photosynthetic performance in wheat. *Plant Physiol. Biochem.* 160, 341–351. <https://doi.org/10.1016/j.plaphy.2021.01.032>.
- Rajput, V., Minkina, T., Fedorenko, A., Sushkova, S., Mandzhieva, S., Lysenko, V., Duplii, N., Fedorenko, G., Dvadnenko, K., Ghazaryan, K., 2018. Toxicity of copper oxide nanoparticles on spring barley (*Hordeum sativum* distichum). *Sci. Total Environ.* 645, 1103–1113. <https://doi.org/10.1016/j.scitotenv.2018.07.211>.
- Rajput, V.D., Minkina, T., Fedorenko, A., Chernikova, N., Hassan, T., Mandzhieva, S., Sushkova, S., Lysenko, V., Soldatov, M.A., Burachevskaya, M., 2021. Effects of zinc oxide nanoparticles on physiological and anatomical indices in spring barley tissues. *Nanomaterials* 11, 1722. <https://doi.org/10.3390/nano11071722>.
- Ramadan, T., Sayed, S.A., Abd-Elal, A.K.A., Amro, A., 2022. The combined effect of water deficit stress and TiO2 nanoparticles on cell membrane and antioxidant enzymes in *Helianthus annuus* L. *Physiol. Mol. Biol. Plants* 28, 391–409. <https://doi.org/10.1007/s12298-022-01153-z>.
- Rao, S., Shekhawat, G.S., 2014. Toxicity of ZnO engineered nanoparticles and evaluation of their effect on growth, metabolism and tissue specific accumulation in *Brassica juncea*. *J. Environ. Chem. Eng.* 2, 105–114. <https://doi.org/10.1016/j.jece.2013.11.029>.
- Rausser, W.E., 1999. Structure and function of metal chelators produced by plants: The case for organic acids, amino acids, phytin, and metallothioneins. *Cell Biochem. Biophys.* 31, 19–48. <https://doi.org/10.1007/BF02738153>.
- Rossi, L., Fedenia, L.N., Sharifan, H., Ma, X., Lombardini, L., 2019. Effects of foliar application of zinc sulfate and zinc nanoparticles in coffee (*Coffea arabica* L.) plants. *Plant Physiol. Biochem.* 135, 160–166. <https://doi.org/10.1016/j.plaphy.2018.12.005>.
- Sabar, M., Gagliardi, D., Balk, J., Leaver, C.J., 2003. ORFB is a subunit of F₁F₀-ATP synthase: insight into the basis of cytoplasmic male sterility in sunflower. *EMBO Rep.* 4, 381–386. <https://doi.org/10.1038/sj.embor.embor800>.
- Salehi, H., Chehregani Rad, A., Sharifan, H., Raza, A., Varshney, R.K., 2022. Aerially applied zinc oxide nanoparticle affects reproductive components and seed quality in fully grown bean plants (*Phaseolus vulgaris* L.). *Front. Plant Sci.* 12, 808141. <https://doi.org/10.3389/fpls.2021.808141>.
- Salehi, H., De Diego, N., Chehregani Rad, A., Benjamin, J.J., Trevisan, M., Lucini, L., 2021. Exogenous application of ZnO nanoparticles and ZnSO₄ distinctly influence the metabolic response in *Phaseolus vulgaris* L. *Sci. Total Environ. Ment.* 778, 146331. <https://doi.org/10.1016/j.scitotenv.2021.146331>.
- Salvato, F., Havelund, J.F., Chen, M., Rao, R.S.P., Rogowska-Wrzzesinska, A., Jensen, O. N., Gang, D.R., Thelen, J.J., Møller, I.M., 2014. The potato tuber mitochondrial proteome. *Plant Physiol.* 164, 637–653. <https://doi.org/10.1104/pp.113.229054>.
- Sani, M.N.H., Amin, M., Siddique, A.B., Nasif, S.O., Ghaley, B.B., Ge, L., Wang, F., Yong, J.W.H., 2023. Waste-derived nanobiochar: a new avenue towards sustainable agriculture, environment, and circular bioeconomy. *Sci. Total Environ.* 905, 166881. <https://doi.org/10.1016/j.scitotenv.2023.166881>.
- Savchenko, T., Tikhonov, K., 2021. Oxidative stress-induced alteration of plant central metabolism. *Life* 11, 304. <https://doi.org/10.3390/111040304>.
- Singh, D., Chauhan, S.K., 2011. Organic acids of crop plants in aluminium detoxification. *Curr. Sci.* 100, 1509–1515.
- Singh, A., Prasad, S.M., Singh, S., 2018. Impact of nano ZnO on metabolic attributes and fluorescence kinetics of rice seedlings. *Environ. Nanotechnol. Monit. Manag.* 9, 42–49. <https://doi.org/10.1016/j.enmm.2017.11.006>.
- Sipari, N., Lihavainen, J., Shapiguzov, A., Kangasjärvi, J., Keinänen, M., 2020. Primary metabolite responses to oxidative stress in early-senescing and paraquat resistant *Arabidopsis thaliana* rcd1 (Radical-Induced Cell Death1). *Front. Plant Sci.* 11, 194. <https://doi.org/10.3389/fpls.2020.00194>.
- Song, W., Zhang, Jinyang, Guo, J., Zhang, Jinhua, Ding, F., Li, L., Sun, Z., 2010. Role of the dissolved zinc ion and reactive oxygen species in cytotoxicity of ZnO nanoparticles. *Toxicol. Lett.* 199, 389–397. <https://doi.org/10.1016/j.toxlet.2010.10.003>.
- Suzuki, N., Koussevitzky, S., Mittler, R., Miller, G., 2012. ROS and redox signalling in the response of plants to abiotic stress: ROS and redox signalling in plants. *Plant Cell Environ.* 35, 259–270. <https://doi.org/10.1111/j.1365-3040.2011.02336.x>.
- Tombuloglu, H., Slimani, Y., Tombuloglu, G., Almessiere, M., Sozeri, H., Demir-Korkmaz, A., AlShammari, T.M., Baykal, A., Ercan, I., Hakeem, K.R., 2019a. Impact of calcium and magnesium substituted strontium nano-hexaferite on mineral uptake, magnetic character, and physiology of barley (*Hordeum vulgare* L.). *Ecotoxicol. Environ. Saf.* 186, 109751. <https://doi.org/10.1016/j.ecoenv.2019.109751>.
- Tombuloglu, H., Slimani, Y., Tombuloglu, G., Demir Korkmaz, A., Baykal, A., Almessiere, M., Ercan, I., 2019b. Impact of superparamagnetic iron oxide nanoparticles (SPIONs) and ionic iron on physiology of summer squash (*Cucurbita pepo*): a comparative study. *Plant Physiol. Biochem.* 139, 56–65. <https://doi.org/10.1016/j.plaphy.2019.03.011>.
- Tombuloglu, H., Slimani, Y., Tombuloglu, G., Almessiere, M., Baykal, A., Ercan, I., Sozeri, H., 2019c. Tracking of NiFe₂O₄ nanoparticles in barley (*Hordeum vulgare* L.) and their impact on plant growth, biomass, pigmentation, catalase activity, and mineral uptake. *Environ. Nanotechnol. Monit. Manag.* 11, 100223. <https://doi.org/10.1016/j.enmm.2019.100223>.
- Tombuloglu, G., Tombuloglu, H., Slimani, Y., Almessiere, M.A., Baykal, A., Bostancioglu, S.M., Kirat, G., Ercan, I., 2024. Effects of foliar iron oxide nanoparticles (Fe₃O₄) application on photosynthetic parameters, distribution of mineral elements, magnetic behaviour, and photosynthetic genes in tomato (*Solanum lycopersicum* var. cerasiforme) plants. *Plant Physiol. Biochem.* 210, 108616. <https://doi.org/10.1016/j.plaphy.2024.108616>.
- Vafaie Moghadam, A., Iranbakhsh, A., Saadatmand, S., Ebad, M., Oraghi Ardebili, Z., 2022. New insights into the transcriptional, epigenetic, and physiological responses to zinc oxide nanoparticles in *Datura stramonium*; potential species for phytoremediation. *J. Plant Growth Regul.* 41, 271–281. <https://doi.org/10.1007/s00344-021-10305-6>.
- Voloshina, M., Rajput, V., Minkina, T., Vechkanov, E., Mandzhieva, S., Mazarji, M., Churyukina, E., Plotnikov, A., Krepakova, M., Wong, M., 2022. Zinc oxide nanoparticles: Physiological and biochemical responses in barley (*Hordeum vulgare* L.). *Plants* 11, 2759. <https://doi.org/10.3390/plants11202759>.
- Wan, J., Wang, R., Rutting, Wang, Ruling, R., Ju, Q., Wang, Y., Xu, J., 2019. Comparative physiological and transcriptomic analyses reveal the toxic effects of ZnO nanoparticles on plant growth. *Environ. Sci. Technol.* 53, 4235–4244. <https://doi.org/10.1021/acs.est.8b06641>.
- Wang, X., Ma, Y., Huang, C., Wan, Q., Li, N., Bi, Y., 2008. Glucose-6-phosphate dehydrogenase plays a central role in modulating reduced glutathione levels in reed callus under salt stress. *Planta* 227, 611–623. <https://doi.org/10.1007/s00425-007-0643-7>.
- Wang, X., Yang, X., Chen, S., Li, Q., Wang, W., Hou, C., Gao, X., Wang, L., Wang, S., 2016. Zinc oxide nanoparticles affect biomass accumulation and photosynthesis in *Arabidopsis*. *Front. Plant Sci.* 6. <https://doi.org/10.3389/fpls.2015.01243>.
- Wang, S., Zhang, Y., Song, Q., Fang, Z., Chen, Z., Zhang, Yamin, Zhang, Lili, Zhang, Lin, Niu, N., Ma, S., Wang, J., Yao, Y., Hu, Z., Zhang, G., 2018. Mitochondrial dysfunction causes oxidative stress and tapetal apoptosis in chemical hybridization reagent-

- induced male sterility in wheat. *Front. Plant Sci.* 8, 2217. <https://doi.org/10.3389/fpls.2017.02217>.
- Wu, B., Zhu, L., Le, X.C., 2017. Metabolomics analysis of TiO₂ nanoparticles induced toxicological effects on rice (*Oryza sativa* L.). *Environ. Pollut.* 230, 302–310. <https://doi.org/10.1016/j.envpol.2017.06.062>.
- Xu, J., Maki, D., Stapleton, S.R., 2003. Mediation of cadmium-induced oxidative damage and glucose-6-phosphate dehydrogenase expression through glutathione depletion. *J. Biochem. Mol. Toxicol.* 17, 67–75. <https://doi.org/10.1002/jbt.10062>.
- Yang, Z., Chen, J., Dou, R., Gao, X., Mao, C., Wang, L., 2015. Assessment of the phytotoxicity of metal oxide nanoparticles on two crop plants, maize (*Zea mays* L.) and rice (*Oryza sativa* L.). *IJERPH* 12, 15100–15109. <https://doi.org/10.3390/ijerph121214963>.
- Yang, Y., Fu, Z., Su, Y., Zhang, X., Li, G., Guo, J., Que, Y., Xu, L., 2014. A cytosolic glucose-6-phosphate dehydrogenase gene, *ScG6PDH*, plays a positive role in response to various abiotic stresses in sugarcane. *Sci. Rep.* 4, 7090. <https://doi.org/10.1038/srep07090>.
- Yasmeen, F., Raja, N.L., Razaq, A., Komatsu, S., 2017. Proteomic and physiological analyses of wheat seeds exposed to copper and iron nanoparticles. *Biochim. Biophys. Acta Proteins Proteom.* 1865, 28–42. <https://doi.org/10.1016/j.bbapap.2016.10.001>.
- Yoshida, K., Hisabori, T., 2016. Adenine nucleotide-dependent and redox-independent control of mitochondrial malate dehydrogenase activity in *Arabidopsis thaliana*. *Biochim. Biophys. Acta Bioenergy* 1857, 810–818. <https://doi.org/10.1016/j.bbapap.2016.03.001>.
- Zhang, H., Du, W., Peralta-Videa, J.R., Gardea-Torresdey, J.L., White, J.C., Keller, A., Guo, H., Ji, R., Zhao, L., 2018. Metabolomics reveals how cucumber (*Cucumis sativus*) reprograms metabolites to cope with silver ions and silver nanoparticle-induced oxidative stress. *Environ. Sci. Technol.* 52, 8016–8026. <https://doi.org/10.1021/acs.est.8b02440>.
- Zhang, Y., Fernie, A.R., 2018. On the role of the tricarboxylic acid cycle in plant productivity: The role of TCA in the plant productivity. *J. Integr. Plant Biol.* 60, 1199–1216. <https://doi.org/10.1111/jipb.12690>.
- Zhu, X.F., Zheng, C., Hu, Y.T., Jiang, T., Liu, Y., Dong, N.Y., Yang, J.L., Zheng, S.J., 2011. Cadmium-induced oxalate secretion from root apex is associated with cadmium exclusion and resistance in *Lycopersicon esulentum*: oxalate secretion and cadmium exclusion. *Plant Cell Environ.* 34, 1055–1064. <https://doi.org/10.1111/j.1365-3040.2011.02304.x>.
- Zhu, J., Zou, Z., Shen, Y., Li, J., Shi, S., Han, S., Zhan, X., 2019. Increased ZnO nanoparticle toxicity to wheat upon co-exposure to phenanthrene. *Environ. Pollut.* 247, 108–117. <https://doi.org/10.1016/j.envpol.2019.01.046>.